November 2022

Recognition of Modern Modulated Waveforms with Applications to ABMS and VDATS Test Program Set Development

Sylwester Sobolewski
University of South Florida

Recognition of Modern Modulated Waveforms with Applications to ABMS and VDATS Test Program Set Development

by

Sylwester Sobolewski

A dissertation submitted in partial fulfillment
of the requirements for the degree of
Doctor of Philosophy
Department of Electrical Engineering
College of Engineering
University of South Florida

Major Professor: Ravi Sankar, Ph.D.
Nasir Ghani, Ph.D.
Ismail Uysal, Ph.D.
Srinivas Katkoori, Ph.D.
Leslaw Skrzypek, Ph.D.

Date of Approval:
November 22, 2022

Keywords: Automatic Modulation Recognition, Feature Extraction Techniques, Analog Modulations, Digital Modulations, Principal Component Analysis

Dedication

This dissertation is dedicated to my parents and all my family and friends who supported and encouraged me from near and far during my studies.

Acknowledgments

I would like to sincerely thank my major research advisor Distinguished Prof. Ravi Sankar, for providing constant support, guidance and patience throughout my research. I would also like to thank my professional technical advisor and co-author of several publications, Air Force VDATS Program Team Leader, Principal System Engineer William Larry Adams Jr for his technical expertise and direction pertinent to this research project and all the doctoral committee members, whose knowledge and constructive feedback allowed to improve my research abilities.

Table of Contents

List of Tables

List of Figures

Abstract

A newly developed, near real-time, well-performing and potentially universally applicable Automatic Modulation Recognition (AMR) technique for discrimination of numerous modern modulated waveforms found in commercial as well as military communication systems applicable to the new Air Force's Advanced Battle Management & Surveillance (ABMS) framework as well as Versatile Depot Automatic Test Station (VDATS) Test Program Set (TPS) development is presented. It involves generating complex feature vectors composed of High-Order Direct Cumulant, Cyclostationary and Fourier of Wavelet Transform features created with the help of Principal Component Analysis and Variance Data Compression.

Twelve modulated waveforms are used to evaluate the performance of the expanded feature vectors: eight commercial modulated waveforms [Quaternary Amplitude Shift Keying (QASK), Quaternary Frequency Shift Keying (QFSK), Quaternary Phase Shift Keying (QPSK), 16-Point Quadrature Amplitude Modulation (QAM-4,4), Gaussian Minimum Shift Keying (GMSK), Frequency Quadrature Amplitude Modulation (FQAM), Filter Bank Multi Carrier (FBMC) and Universal Filtered Multi Carrier (UFMC)], (Cosine) Binary Offset Carrier - BOC(1,1) - waveforms used in the European Galileo Navigation System and three waveforms utilized in defense military systems [Quaternary Linear Frequency Modulation (QLFM), Quaternary Pulse Width and Pulse Position Modulations (QPWM and QPPM)]. Generated complex feature vectors are categorized with the help of a neural network and compared with corresponding library feature patterns.

The presented experimental results are rather unprecedented in the literature since to the best of the authors knowledge, no research team has considered such a varied and comprehensive

modulation format test set of waveforms in a single study. There have been some hierarchical modulation classifications schemes proposed in the earlier research dating to the early 2000s; however, their modulation format test sets were very limited and the classification performance for those that could be compared to the current research was dramatically lower. Also, there have been some attempts to generate the required probabilities for the other class of maximum-likelihood techniques generating very complex mathematical formulas in numerous cases for a handful of modulation formats. The latest research also addresses some of the feature-based non-hierarchical techniques but again the techniques presented are detached from one another and modulation format test sets are usually limited too. The research presented in this work gives a convenient and effective non-hierarchical method for modulation format classification that is potentially universally applicable to any conceivable modulated waveform that can be represented in the time domain while keeping the computational complexity reasonable so as to be applicable for real-time implementation in the future communications systems. The study described which feature-based techniques are broadly applicable and of these which are actually performing best and are readily suitable for easy implementation.

Chapter 1: Introduction

1.1 Background

In the current era of ubiquitous communication signals coming from various sources and tremendous proliferation of personal, commercial and military devices it becomes increasingly difficult to manage these systems and appropriately allocate the necessary resources. The concept of Internet of Things (IoT), or Internet of Everything (IoE), puts a great strain on the modern communications networks and increasingly complex and clever methods must be implemented to allow for constantly growing data rate, bandwidth, capacity and speed requirements. The newest 5th Generation (5G) New Radio communication systems may be one of the best examples.

Additionally, the United States Air Force is creating its own communications framework to manage military's forces in war. This emerging overarching system, planned to reach full maturity in the 2040s, is called Advanced Battle Management & Surveillance (ABMS) [1]. It is military equivalent of the commercial Internet of Things / Everything (IoT/IoE) and 5th Generation (5G) communications standards and is expected to replace the Air Force's Airborne Warning and Control System (AWACS) E-3A and Joint Surveillance Target Attack Radar System (JSTARS) E-8C platforms and the Situational Awareness Data Link (SADL) inter-platform communications network currently implementing Joint All-Domain Command and Control (JADC2) functions [2].

To address all of such communication systems demands, although on a much smaller scale than currently, the concept of Automatic Modulation Recognition (AMR) was started being implemented more than 3 decades ago in connection with Cognitive Software Radios research.

The main paradigm of operation of cognitive radios is the cognition cycle based on model-based reasoning [3]. AMR utilizes artificial intelligence to decide on the resources required by examining the available spectrum, network demand and numerous other parameters to help the intelligent communication receiver perform at its best.

1.2 Applications of Automatic Modulation Recognition / Signal Detection

Potential applications of AMR and Signal Detection algorithms / techniques in the current connected world are tremendous. They are useful and quite often outright necessary whenever it is needed to determine the source and nature of the incoming received communications signals. Clearly, they are just as importantly applicable to both commercial and military signals whose multitude and complexity is only continuously increasing. Two particular applications this study focused on were the newly developed Air Force ABMS communications framework and VDATS TPS Development.

1.2.1 Newly Developed U.S. Air Force ABMS Framework

The U.S. Air Force is currently developing a brand-new Advanced Battle Management & Surveillance (ABMS) communications framework which will initially complement and eventually replace the currently operating SADL communications network utilizing Link 16 standard, a military tactical data link incorporating periodic time-slotted messaging scheme network as shown in the operational schematic of Figure 1.1, with a new and improved Multifunction Advanced Data Link (MADL).

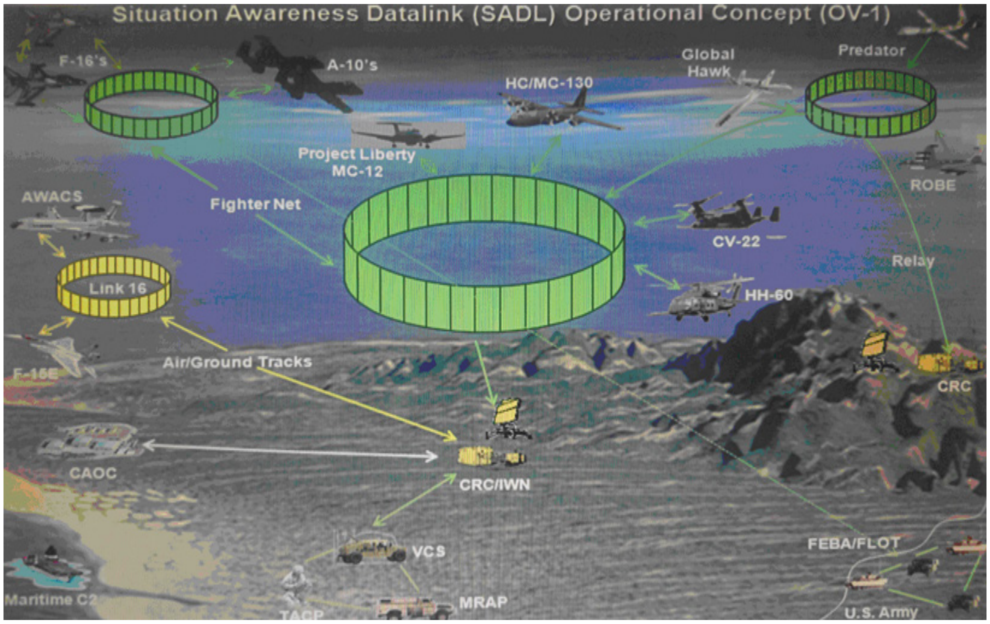

Figure 1.1 Situational Awareness Data Link Operational Concept Schematic

In addition, a new more secure data link standard is being developed by NATO nations, called Link 22, which is expected to initially complement Link 16 and eventually most likely replace it in the new developed ABMS system, an expected natural successor of SADL. The command-and-control aircraft currently performing the JADC2 functions, E-3A AWACS and E-8C JSTARS, Figure 1.2, are also being gradually phased out and planned to be upgraded to newer platforms. In the case of E-3 the replacement may potentially be Boeing's E-7 Wedgetail beginning in 2027.

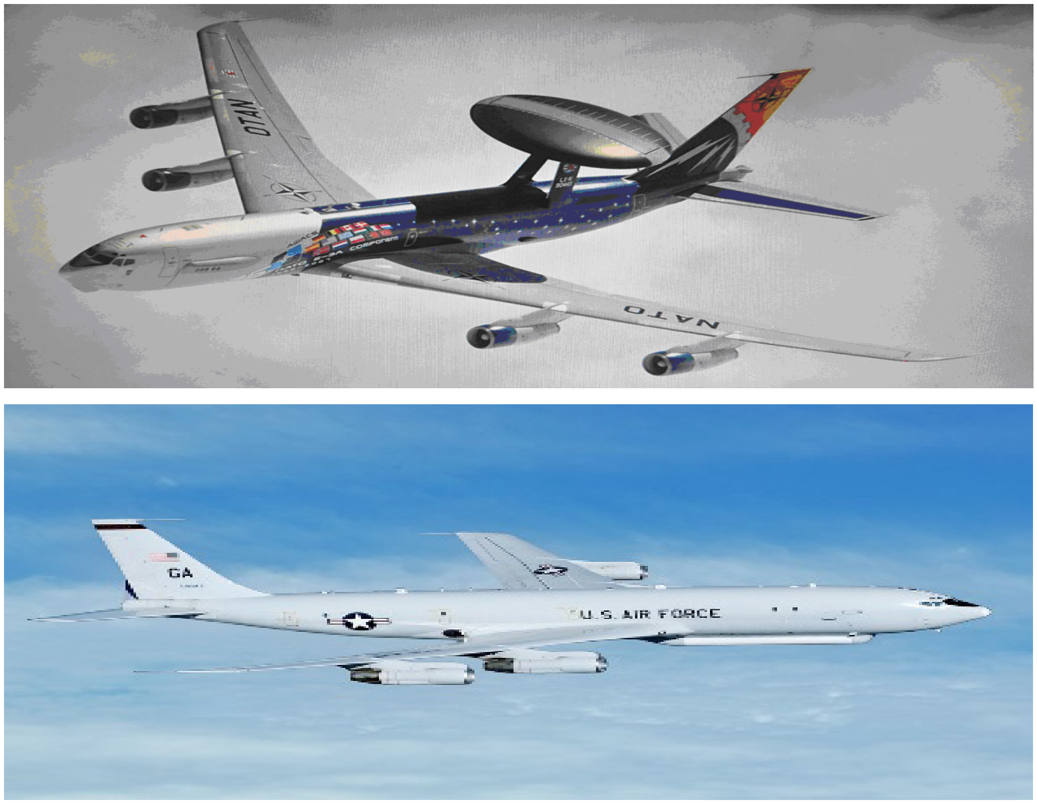

Figure 1.2 Command & Control Aircraft: E-3A (Top), E-8C (Bottom)

1.2.2 VDATS Test Program Set Development

Another application of AMR addressed was the Air Force (AF) Versatile Diagnostic Automatic Test Station (VDATS) TPS Development. The VDATS program has been around for about 15 years, having been started at Robins AFB, GA back in 2007 as a solution to the AF Automatic Test System (ATS) proliferation problem and also addressing the issues of obsolescence and supportability of numerous Test hardware systems [4]. Currently, approximately 140 VDATS units have been fielded across the Air Force, with close to 5,000 Test Program Sets (TPSs) being implemented on the stations and the demand still growing with forecasts to surpass 200 stations in the near future and associated re-hosted testing workloads becoming increasingly varied. The VDATS exists in two core variants: Digital-Analog (DA) and Radio Frequency (RF), as shown in Figure 1.3. In addition, there are around a dozen portable support Roll-Up Racks, depending on particular TPS system being evaluated.

Figure 1.3 VDATS Core Variants: Digital-Analog (DA, Left) and Radio Frequency (RF, Right)

The AMR is undeniably applicable to the current SADL network and even more so to the newly developed MADL network. It can be utilized in any particular military system where signal identification is involved, such as for example, Identification Friend or Foe (IFF), Radar Warning Receivers (RWRs), Precision Navigation and Timing (PNT), Nuclear, Command, Control and Communications (NC3) VHF/UHF Radios utilized in the current SADL network as well as their planned replacements likely to make their way to the newly developed ABMS's MADL network structure.

Most of TPS development work is classified. Thus, it is not easy to determine the exact number of TPSs dealing with signal detection and modulation recognition and the testing procedures addressing these tasks themselves. Some known examples of TPSs involving such functions are AN/ALR-69A RWR, LAK (Link 16 Alaska), AN/ARC-164/-169/-186/-190/-210/-

222/-230 VHF/UHF Radios and AN/APX-113/-125/-126 IFF combined Interrogator and Transponder.

1.3 Motivations and Research Objectives

The motivation for this study has been the desire to find an Automatic Modulation Recognition / Signal Detection algorithm / technique that is potentially universally applicable and identifies most effectively and with a reasonable computational complexity, so as to be applicable for real-time operation, the largest number of signals received, both commercial and military, with a greater bias towards military applications though as to relate more closely with my professional interests in the Department of Defense: Air Force, Navy or Army.

The two main objectives of this study were: 1) Perfecting an AMR technique that could be for certain implemented in the newly developed ABMS framework on various platforms that make up its overall structure, 2) Improving the VDATS and potentially also other testers Test Program Set execution flow to allow for effective implementation of the critical testing procedures supporting a wide variety of warfighter utilized hardware testing requirements.

1.4 Contributions

The contributions of this work were:

1) Development of relatively simple and effective feature vectors readily applicable for discrimination of various modern modulated waveforms in particular those that are likely to be implemented in the newly developed ABMS framework.

2) Implementation of individual CM, CS and FWT techniques, a 3-member CM-CS-FWT varied-technique diversity Majority-Selection-Rule classifier as well as a same-type diversity distributed scheme with several (Up to 7) individual receivers showing performance of the compressed compound feature vectors.

3) Demonstration of the application of the individual and compound feature vectors for a large and varied 12-member set of modulated signals. The outstanding classification performance of these feature vectors as compared to other techniques found in the literature further supports their ability in future communications systems.

4) Description of how the proposed AMR techniques are equally well suitable to be implemented in numerous Test Program Sets that are being executed on VDATS testers where modulation classification and signal detection are being addressed.

1.5 Dissertation Organization

Chapter 2 gives a detailed review of signal detection algorithms: Maximum-Likelihood Based as well as Feature-Based Automatic Modulation Recognition Techniques.

Chapter 3 describes how the best AMR techniques were selected so as to be widely applicable and potentially universal in identifying the examined modulation formats present. An experimental evaluation of the selected techniques performance further justifies their selection.

Chapter 4 analyzes the development of best performing and computationally feasible techniques for near real-time operation. Initially all applicable AMR techniques are identified. Then based on their performance the best ones are singled out as being preferred.

Chapter 5 presents Neural Network training and classification algorithms for evaluation of the proposed AMR techniques.

Chapter 6 gives a comparison of the AMR classification performance of the proposed techniques with the results in the literature. In addition, the modulation format coverage is also addressed.

Chapter 7 provides a summary of this research project as well as any possible improvements and extensions of coverage plus tentative future directions.

Chapter 2: Review of Automatic Modulation Recognition Techniques[1]

The body of research dealing with Automatic Modulation Recognition, sometimes also referred to as signal source detection, can be divided into two general classes: Maximum-Likelihood based and Feature-based techniques.

2.1 Maximum-Likelihood Based Techniques

In a maximum likelihood technique, the classification is treated as a multiple-hypothesis testing problem, with a hypothesis H_i arbitrarily assigned to the *i*th modulation type of *m* possible types with constellation sizes M_i .

The Probability Density Function (PDF) of observed received point X_k , conditioned on the received modulated signal m_i, contains all the information required for classification, that is [5,6]:

$$P(X_k|H_i) = \sum_{j=1}^{M_i} P\left(X_k \middle| a_j^i\right) P\left(a_j^i \middle| H_i\right) \tag{1}$$

where $P\left(X_k \middle| a_j^i\right)$ is the probability density function that the received point was transmitted at *j*th constellation point of *i*th modulation type a_j^i, Conditional Likelihood Function (CLF), and $P\left(a_j^i \middle| H_i\right)$ is the a priori probability density function of constellation point a_j^i given a modulation type m_i . Usually, $P\left(a_j^i \middle| H_i\right) = 1/M_i$. For observed received signal vector X = $[X_1 X_2 \cdots X_L]$, the pdf of modulation type m_i , likelihood function (LF), is:

$$LF^i = P(X|H_i) = \prod_{n=1}^{L} P(X_n|H_i) \equiv L(X|H_i) \tag{2}$$

The Maximum Likelihood (ML) classifier reports the *j*th modulation type based on the observation

[1] Portions of this chapter were published in [22,27]. Permissions are included in Appendix A.

whenever $L(X|H_j) > L(X|H_i)$, $j \neq i, \; j,i = 1,2, \ldots, m$, that is, chooses the modulation type with the largest likelihood function.

The classification decision is made, for two-hypothesis problem, as:

$$LR = \frac{LF_Z^1 : H_1}{LF_Z^2 : H_2} \gtrless \eta_z \tag{3}$$

where η_z is a threshold and the left side of the above inequality is referred to as the likelihood ratio and the test is called: average likelihood ratio test (Z = ALRT), generalized likelihood ratio test (Z = GLRT) or hybrid likelihood ratio test (Z = HLRT), depending on the method used to compute the LF, the model chosen for unknown quantities. The inequality can also be extended to multiple classes (hypotheses).

2.1.1 Average Likelihood Ratio Test

The expression for Likelihood Function (LF) of ALRT in a compact notation can be written as [6]:

$$LF_{ALRT}^i = \sum_{i=1}^{M_i} P(x(t)|v_i, H_i)\, P(v_i|H_i) \tag{4}$$

where v_i is a vector of unknown quantities treated as random variables with certain *pdf*'s.

2.1.2 Generalized Likelihood Ratio Test

The expression for LF of GLRT can be written as:

$$LF_{GLRT}^i = \max_{v_i} \; P(x(t)|v_i, H_i) \tag{5}$$

where v_i is a vector of unknown parameters modeled as deterministic values.

2.1.3 Hybrid Likelihood Ratio Test

For the HLRT, the combination of ALRT and GLRT approaches, the Likelihood Function is given by:

$$LF_{HLRT}^i = \max_{v_{i1}} \sum_{i2=1}^{M_i} P(x(t)|v_{i1}, v_{i2}, H_i)\, P(v_{i2}|H_i) \tag{6}$$

where v_{i1} and v_{i2} are vectors of unknown quantities modeled as deterministic values and random variables, respectively. Usually, v_{i1} and v_{i2} consist of parameters and data symbols, respectively.

The three maximum likelihood approaches described above using exact (ideal) values of pdf's are said to be optimal, they maximize the probability of correct classification. When the expressions for the pdf's are approximate and assume prior information like the symbol rate and SNR, the approaches are said to be sub-optimal.

2.2 Feature-Based Techniques

In a Feature-based technique, the classification is performed by comparing the received modulated waveform with a pre-defined set in the existing library of waveforms (Feature vectors). Numerous specific techniques in this category have been devised in the literature, the most significant are the following.

2.2.1 Signal Statistics Technique

In the Signal Statistics technique, the feature vectors are constructed from quantities computed directly from the modulated signal itself such as [7-9]:

1) Standard deviation of normalized-centered instantaneous direct amplitude of waveform:

$$\sigma_{da} = \sqrt{(1/N)(\sum_{i=1}^{N} A_{cn}^2(i)) - \left((1/N)\ \sum_{i=1}^{N} A_{cn}(i)\right)^2} \quad (7)$$

2) Standard deviation of normalized-centered instantaneous absolute amplitude:

$$\sigma_{aa} = \sqrt{(1/N)(\sum_{i=1}^{N} A_{cn}^2(i)) - \left((1/N)\ \sum_{i=1}^{N} |A_{cn}(i)|\right)^2} \quad (8)$$

3) Kurtosis of normalized instantaneous amplitude:

$$\mu_{42}^{a} = E[A_n^4(i)]/\{E[A_n^2(i)]\}^2 \quad (9)$$

4) Standard deviation of absolute value of normalized instantaneous frequency of waveform:

$$\sigma_{af} = \sqrt{(1/N)(\sum_{i=1}^{N} f_n^2(i)) - \left((1/N)\ \sum_{i=1}^{N} |f_n(i)|\right)^2} \quad (10)$$

where $f_n(i) = f_c(i)/R_b$ and $f_c(i) = f(i) - mean(f)$

5) Kurtosis of normalized instantaneous frequency:

$$\mu_{42}^{f} = E[\, f_n^4(i)\,]/\{E[\, f_n^2(i)\,]\}^2 \tag{11}$$

6) Standard deviation of instantaneous direct phase of waveform:

$$\sigma_{dp} = \sqrt{(1/N)(\,\sum_{i=1}^{N} \varphi^2(i)) - \Big((1/N)\ \sum_{i=1}^{N} \varphi(i)\Big)^2} \tag{12}$$

7) Standard deviation of instantaneous absolute phase of waveform:

$$\sigma_{ap} = \sqrt{(1/N)(\,\sum_{i=1}^{N} \varphi^2(i)) - \Big((1/N)\ \sum_{i=1}^{N} |\varphi(i)|\Big)^2} \tag{13}$$

8) Standard deviation of instantaneous direct unwrapped phase of symbol in waveform σ_{dps}

9) Standard deviation of instantaneous absolute unwrapped phase of symbol in waveform σ_{aps}

10) Maximum value of power spectral density of normalized-centered instantaneous amplitude:

$$\gamma_{max} = max\ |DFT(A_{cn}(i))|^2 \tag{14}$$

11) Total normalized power from Power Spectral Density of the waveform P_{total_norm}

(Highest PSD amplitude = 1)

2.2.2 Higher Order Statistics (Cumulants) Technique

The second Feature based technique is Higher Order Statistics, the most common of which are Cumulants of any order *n* [10-15]. They can be easily calculated from the following recursive Moment-to-Cumulant formula:

$$C_n = M_n - \sum_{m=1}^{n-1} \frac{(n-1)!}{(m-1)!\cdot(n-m)!} C_m M_{n-m} \tag{15}$$

where a central moment *M* of order *n* (about mean μ) is defined as:

$$M_n = \int_{-\infty}^{+\infty} (x-\mu)^n \cdot p_x(x)dx = \sum_{n=1}^{N} (x-\mu)^n[k] \cdot p_x\big(x(k)\big) = \frac{1}{N}\sum_{n=1}^{N} (x-\mu)^n[k] \tag{16}$$

2.2.3 Cyclostationary Features Technique

The third technique takes advantage of the fact that many time signal waveforms / processes can be modeled as cyclostationary rather than stationary due to the underlying periodicities of the signals [16-20]. For such processes both their means and autocorrelations are periodic. A Spectral Correlation Function (SCF), also known as Spectral Correlation Density (SCD), can be obtained from the Fourier transform of the cyclic autocorrelation.

Cyclic spectral analysis deals with second order transformations of a function and its spectral representation. A time waveform (process) *x(t)* is said to exhibit second order periodicity if spectral components of *x(t)* exhibit temporal correlation. A wide sense stationary process *x(t)* has time invariant autocorrelation function:

$$R_x(t,\tau) = E\{x(t)x(t-\tau)^*\} \quad \text{and} \quad R_x(t,\tau) = R_x(\tau)\ \forall t \tag{17}$$

The Wiener relationship relates autocorrelation and power spectral density:

$$S_x(f) = F\{R_x(\tau)\} = \int_{-\infty}^{+\infty} R_x(\tau)\, e^{-j2\pi f\tau} d\tau \tag{18}$$

A cyclostationary process *x(t)* (in wide sense) has periodic mean and autocorrelation function for some period T_o. The Wiener relationship can be established for cyclostationary processes too and is called cyclic Wiener relation:

$$S_x^\alpha(f) = F\{R_x^\alpha(\tau)\} = \int_{-\infty}^{+\infty} R_x^\alpha(\tau)\, e^{-j2\pi f\tau} d\tau \tag{19}$$

$$\text{where} \qquad \alpha = n/T_o\,, n = \pm 1, \pm 2, \pm 3, \ldots.$$

This relation leads to discrete spectral correlation function (SCF) [19]:

$$S_x^\alpha(f) = \frac{1}{N}\frac{1}{T}\sum_{n=0}^{N} X_T\left(n, f+\frac{\alpha}{2}\right) X_T^*\left(n, f-\frac{\alpha}{2}\right) \tag{20}$$

$$\text{where} \qquad X_T(n,f) = \int_{n-T/2}^{n+T/2} x(u) e^{-j2\pi f u} du$$

which is normalized to obtain the Spectral Coherence (SC):

$$C_x^{\alpha}(f) = \frac{S_x^{\alpha}(f)}{\left[S_x^0(f+\alpha/2)^* S_x^0(f-\alpha/2)\right]^{1/2}} \tag{20a}$$

2.2.4 Multifractal Features Technique

The fourth feature-based technique utilizes multiple fractal dimensions of potentially non-linearly generated modulated signals that can be treated as one-dimensional functions of time with statistically irregular waveforms [21]. Fractal theory has been widely used in signal processing to analyze voice, image and radar signals. A fractal describes the degree of roughness or meandering of a data sequence and constitutes a rough or fragmented shape that can be partitioned, with each of the parts being roughly a reduced-size copy of whole. Fractals are usually self-similar and independent of scale. Fractal dimensions extracted from signals contain information about magnitude, frequency and phase of signals and can discriminate numerous modulation formats. They are useful features for classification and are insensitive to noise. Single fractal dimension may not describe and discriminate signals because fractal dimensions can only characterize self-similarity in perfect scenarios; real signals are merely semi-fractals and have inhomogeneous scaling properties. Thus, a set of fractal dimensions, not only one, must be used to describe modulated signals. The generalized fractal dimension D_q is defined as [21]:

$$D_q = \begin{cases} \frac{1}{q-1} \lim_{\delta \to 0} \frac{ln\left(N(q,\delta)\right)}{\ln(\delta)}, & q \neq 1 \\ \lim_{\delta \to 0} \frac{\sum p_i \cdot ln(p_i)}{ln(\delta)}, & q = 1 \end{cases} \tag{21}$$

The modified correlation integral method is a convenient means to estimate generalized dimension D_q. The qth order correlation integral for a discrete fractal set is defined as:

$$C(q,r) = \left\{\frac{1}{N_m} \sum_{i=1}^{N_m} \left[\frac{1}{N_m} \sum_{j=1}^{N_m} H\left(r - r_{ij}\right)\right]^{q-1}\right\}^{\frac{1}{q-1}} \tag{22}$$

In practice, the generalized dimension D_q is calculated from the slope of approximately linear central segment of the curve $\ln\big(C(q,r)\big) \sim \ln(r)$.

2.2.5 Fourier Transform of Continuous Wavelet Transform Technique

The fifth technique first determines the Continuous Wavelet Transform of each modulated data waveform and then uses the magnitude of the Fourier Transform of the result to generate a feature vector to be used in subsequent pattern recognition.

The continuous wavelet transform of a continuous, square-integrable function *x(t)* at a scale a > 0 and translational value $b \in R$ is expressed by:

$$X_w(a,b) = \frac{1}{\sqrt{|a|}} \int_{-\infty}^{+\infty} x(t)\psi^*\left(\frac{t-b}{a}\right) dt \tag{23}$$

where $\psi(t)$ is a continuous function in both the time domain and the frequency domain called the mother wavelet and * represents operation of complex conjugate. This technique was proposed by the authors of this study [22].

2.2.6 Other Early Feature Based Techniques

Couple of other Feature-based techniques have been developed in the first dozen years of the AMR research, 1988-2000; however, as will be seen in later chapters they were not considered further due to their very limited applicability in identifying various modulation formats. The first of these was the Digital Wavelet Transform (DWT) technique with applicability only to MPSK and MFSK formats [23]. The second, Constellation Shape technique, only applicable to Digital modulation formats [24]. The third, Zero-Crossing technique, which did not have any waveform amplitude discrimination [25]. And finally, the Radon Transform technique which only applied to square or diamond shaped constellations [26].

Chapter 3: Selection of Widely Applicable Potentially Universal AMR Techniques

One of the main objectives of this study was to develop AMR techniques that were applicable to the largest possible set of modulation formats that could be conceived. This chapter addresses this objective.

3.1 Selecting Large and Varied Set of Modulation Formats to Classify

A thorough literature survey has been performed in order to accomplish the task of identifying what modulation formats have been addressed in the body of research on AMR and source detection. Table 3.1 shows the formats used by various authors in this research area. From this listing an original modulation format set has been selected including these 5 formats:

1) Quaternary Amplitude Shift Keying (QASK or 4ASK)
2) Quaternary Frequency Shift Keying (QFSK or 4FSK)
3) Quaternary Phase Shift Keying (QPSK or 4PSK)
4) 16-Point Quadrature Amplitude Modulation (16-QAM or QAM-(4,4))
5) Gaussian Minimum Shift Keying (GMSK)

Table 3.1 Listing of Modulation Formats Employed in Papers from Initial Literature Survey

AMR Technique	Modulation Formats Covered
Likelihood Function Based	- MPSK, MQAM [5] - B/Q/8/16PSK, 16/32/64QAM, V.29-8/16 [6]
Signal Statistics	- 4ASK, 2/4FSK, 2/4PSK, 16/64QAM, [7] - AM, FM, 2/4FSK, B/QPSK, 2/4ASK, DSB, USB, LSB, VSB [8] - 2/4ASK, 2/4PSK, 2/4FSK [9]

Table 3.1 (Continued)

Higher Order Statistics (Cumulants, Kurtosis, etc)	- 2/4/8/16-PSK, 8/32-QAMstar, 16/64/256-QAM, 16/32/64-QAM, 8/16-V.29 [10] - 2/4-PSK, 16/64-QAM [11] - B/Q-PSK, 16/64-QAM [12] - 2/4/8/16-ASK, B/Q/8/16-PSK, 4/16/64/256-QAM, 8/16/32/64-QAMstar [13] - 4/8-ASK, B/Q/8-PSK, 16/64/256-QAM [14] - MASK/MPAM, B/Q/8-PSK, MQAM, V.29/32 [15]
Cyclostationary features	- B/Q-PSK, BFSK, MSK [16] - B/QPSK, FSK, MSK [17] - AM, B/Q-PSK, FSK, MSK [18,19] - 1-carrier TDMA (GMSK), 1-carrier CDMA (QPSK DS/SS), OFDM (MPSK, MQAM) [20]
Multifractal features	- CW (Continuous Sine Wave), BFSK, BPSK, 4-ASK, 16-QAM [21]
Digital Wavelet Transform	- MPSK, MFSK [23]
Constellation shape	- 8PSK, 8/16QAM, V.29, V.29-Fallback [24]
Zero crossings	- Single-Tone (CW/MPSK) & Multi-Tone (MFSK) – Constant Envelope [25]
Radon transform	- MQAM (4/16/64/256) [26]

In subsequent research, 3 additional modulation formats employed particularly in defense military communications systems have been added [22]:

6) Quaternary Linear Frequency Modulation (QLFM)

7) Quaternary Pulse Width Modulation (QPWM)

8) Quaternary Pulse Position Modulations (QPPM)

In the latest research, first the format utilized in the new European Navigation System GALILEO was added:

9) Binary Offset Carrier – BOC(1,1)

Then 3 additional formats used in the new 5G communications standard for a total of 12 modulation formats [27-31]:

10) Frequency Quadrature Amplitude Modulation (FQAM)

11) Filter Bank Multi Carrier (FBMC)

12) Universal Filtered Multi Carrier (UFMC)

3.1.1 Quaternary Amplitude Shift Keying Modulation Format

Amplitude Shift Keying (ASK) is a form of amplitude modulation which represents digital data as variations of amplitude of a carrier wave:

$$x(t) = \sum_{n=-\infty}^{\infty} v(n) \cdot h_t(t - nT_s) \quad \text{where} \quad v_i = \frac{2A}{L-1} i - A, \quad i = 0,1, \dots, L-1 \tag{24}$$

A is the maximum amplitude and L is the number of levels. In the particular case of QASK (4ASK) there are 4 amplitude levels v_i.

3.1.2 Quaternary Frequency Shift Keying Modulation Format

Frequency Shift Keying (FSK) is a form of frequency modulation scheme in which digital information is transmitted through discrete frequency changes of the carrier signal as in:

$$x(t) = \sqrt{2P} \cdot A \cdot exp(j(2\pi f_m t)) \tag{25}$$

where $m = 0,1, \dots, M$. Each bit or symbol duration has a frequency coming from a set of M frequencies. For QFSK (4FSK) there are 4 frequencies utilized.

3.1.3 Quaternary Phase Shift Keying Modulation Format

Phase shift Keying is a digital modulation format which transmits data by changing the phase of constant frequency reference carrier wave. For Quadrature Phase Shift Keying (QPSK) the implementation is as follows:

$$x_n(t) = \sqrt{\frac{2E_s}{T_s}} cos\left(2\pi f_c t + (2n-1)\frac{\pi}{4}\right), \qquad \text{n} = 1,2,3,4 \tag{26}$$

3.1.4 Quadrature Amplitude Modulation Format

Quadrature Amplitude Modulation (QAM) is a digital modulation format where two bit streams (In-Phase and Quadrature) are transmitted by changing the amplitudes of two carrier waves using the ASK format previously described. The two carrier waves have the same frequency but are out of phase with each other by 90° (Orthogonality or quadrature) expressed as:

$$x(t) = cos(2\pi f_c t)I(t) + cos\left(2\pi f_c t + \frac{\pi}{2}\right)Q(t) \quad (27)$$

For the particular case of 16-Point Quadrature Amplitude Modulation [16-QAM or QAM-(4,4)] there are a total of 16 amplitude and phase combinations for this format.

3.1.5 Gaussian Minimum Shift Keying Modulation Format

Minimum Shift Keying (MSK) is a form of continuous-phase frequency shift keying where the bits are not encoded as square pulses but instead as half sinusoids expressed as:

$$x(t) = a_I(t)cos\left(\frac{\pi t}{2T}\right)cos(2\pi f_c t) - a_Q(t)sin\left(\frac{\pi t}{2T}\right)sin(2\pi f_c t) \quad (28)$$

where $a_I(t)$ and $a_Q(t)$ encode even and odd information with sequence of square pulses of duration $2T$. For GMSK the MSK waveform is also passed through a Gaussian filter.

3.1.6 Quaternary Linear Frequency Modulation Format

The first of the analog modulations is Linear Frequency Modulation which sweeps the frequency within a symbol duration according to formula:

$$x(t) = A \cdot e^{i2\pi\left(\left(f_o - \frac{\Delta f}{2}\right)t + \frac{\Delta f}{2T}t^2\right)} \quad (29)$$

Here Δf can be either positive or negative; thus, both increasing and decreasing frequency sweeps (chirps) are possible. For the case of Quaternary LFM, there can be two up-chirps and two down-chirps.

3.1.7 Quaternary Pulse Width Modulation Format

In this analog modulation, the pulse occupies either a quarter, a half, three quarters or full symbol duration.

3.1.8 Quaternary Pulse Position Modulation Format

Similar to the previous modulation format but here the quarter-width pulse occupies either of the four quadrants of the symbol duration.

3.1.9 Binary Offset Carrier Modulation Format

Binary Offset Carrier is a digital square subcarrier modulation where a signal is multiplied by rectangular sub-carrier of frequency f_{sc} equal to or greater than chip rate as follows:

$$x(t) = c(t)sign[cos(2\pi f_{sc}t)] \quad \text{with} \quad c(t) = \sum_k c_k h(t - kT_c) \tag{30}$$

where c_k is the code sequence and f_{sc} is the sub-carrier frequency. Thus, the spectrum of the signal is divided into two mirrored parts centered around the carrier. In cosine BOC(1,1) variant, '+1' is encoded as '+1 -1' sequence and '0' as '-1 +1' sequence.

3.1.10 Frequency Quadrature Amplitude Modulation Format

Frequency Quadrature Amplitude Modulation is a combination of Frequency Shift Keying and Quadrature Amplitude Modulation and can be expressed as:

$$x_{m,k}(t) = \sqrt{2P} \cdot A_k \cdot exp(j(2\pi f_m t + \varphi_k)) \cdot p_T(t) \tag{31}$$

where $m = 0,1, \ldots, M_{FSK}$ and $k = 1,2, \ldots, M_{QAM}$. In this study a 16-ary FQAM was used which is a combination of 4-ary FSK (QFSK) and 4-ary QAM [QAM-(2,2)].

3.1.11 Filter Bank Multi Carrier Modulation Format

Filter Bank Multi Carrier (FBMC) modulation was one of the first modulations developed to overcome the limitations of Orthogonal Frequency Division Multiplexing (OFDM) which utilized multiple carriers instead of just one. In OFDM, filtering takes place on the entire band of frequencies; on the other hand, in FBMC individual carriers are filtered.

3.1.12 Universal Filtered Multi Carrier Modulation Format

Universal Filtered Multi Carrier (UFMC) Modulation is similar to FBMC but instead of performing filtering on individual carriers here it is done on groups of sub-carriers. In this study, the setups used involved 16-ary systems of carriers for FBMC and UFMC, with sub-bands of 4 in UFMC.

3.2 Maximum-Likelihood vs. Feature-Based Techniques

It has been noted early in the research that the Feature-based techniques are the preferred class of AMR techniques due to its reliance on known library modulated waveforms which can be easily compared with the one being identified. On the other hand, Maximum-Likelihood techniques are not so great in practice since they are based only on probabilities. It is not easy if at all possible to know all the required probabilities that are needed for a given modulation format's identification.

3.3 Experimental Evaluation of Selected Techniques Performance

As stated earlier, this AMR study initially focused on 5 feature-based techniques due to their potentially universal applicability:

1) Signal Statistics (SS)
2) Higher Order Statistics – Cumulants (CM)
3) Cyclostationary features (CS)
4) Multifractal features (MF)
5) Fourier Transform of Continuous Wavelet Transform (FWT)

As described in the next chapter, SS and MF techniques even though potentially universally applicable were only considered in the earlier part of this research study due to their current problems.

3.3.1 Signal Statistics Technique (SS)

For SS technique the feature vectors for each of the modulation formats consisted of 11 elements as described in Section 2.2.1. In order to obtain all these values, first it was required to generate the modulated waveforms for each of the modulation formats as these quantities derived directly from the modulated waveforms. Examples in Figures 3.1-3.8 show the plots illustrating the calculated quantities for 2 modulation formats QFSK and QLFM. For QFSK the 4 frequencies selected were 2.5, 7.5, 12.5 and 17.5 GHz and for QLFM these were the up and down sweeps (Up-Chirp / Down-Chirp) between 2.5 – 7.5 and 2.5 – 17.5 GHz. Figures 3.1 and 3.5 show In-Phase, Quadrature and Total Amplitude along with the Envelope of the QFSK and QLFM waveforms and are used to obtain features #1-3 listed in Section 2.2.1. Figures 3.2 and 3.6 illustrate determination of features #4 and 5 relating to waveform frequency. Figures 3.3 and 3.7 illustrate quantities pertaining to waveform phase and Figures 3.4 and 3.8 help with quantities #10 and 11 relating to power spectral density of the waveform. This is not a good technique in terms of performance as the shapes of the waveforms are easily distorted with increasing noise and its performance deteriorates quickly. The unavoidable band-limiting in practical communications systems also introduces some waveform distortion.

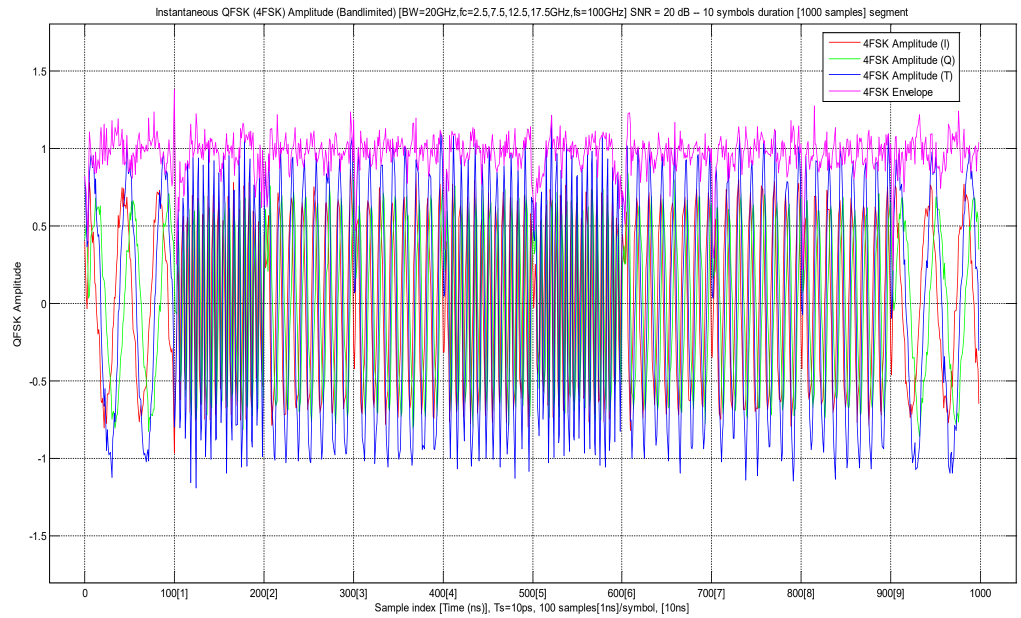

Figure 3.1 Instantaneous Amplitude of QFSK Modulation Format

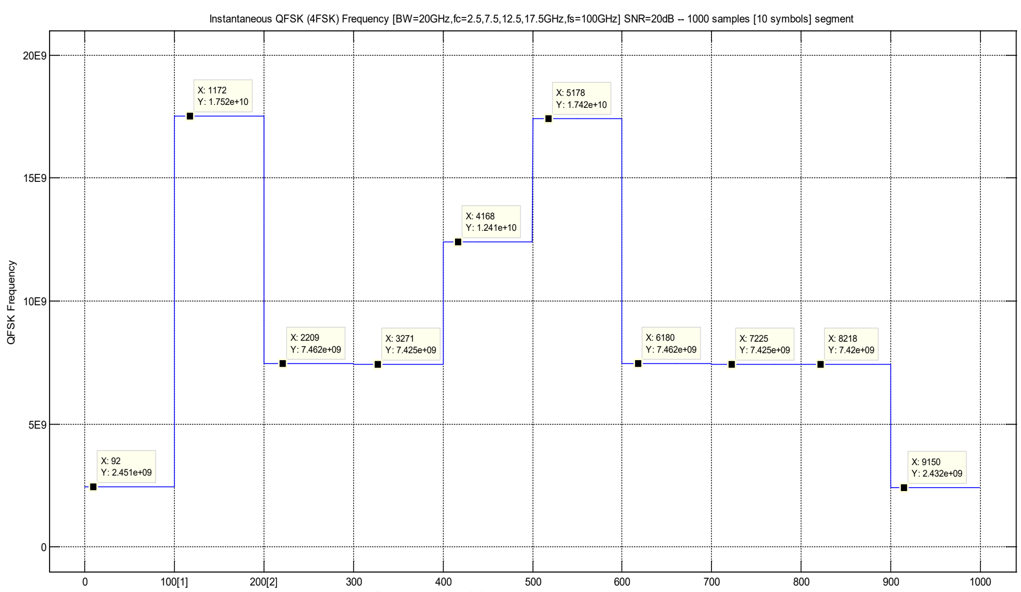

Figure 3.2 Instantaneous Frequency of QFSK Modulation Format

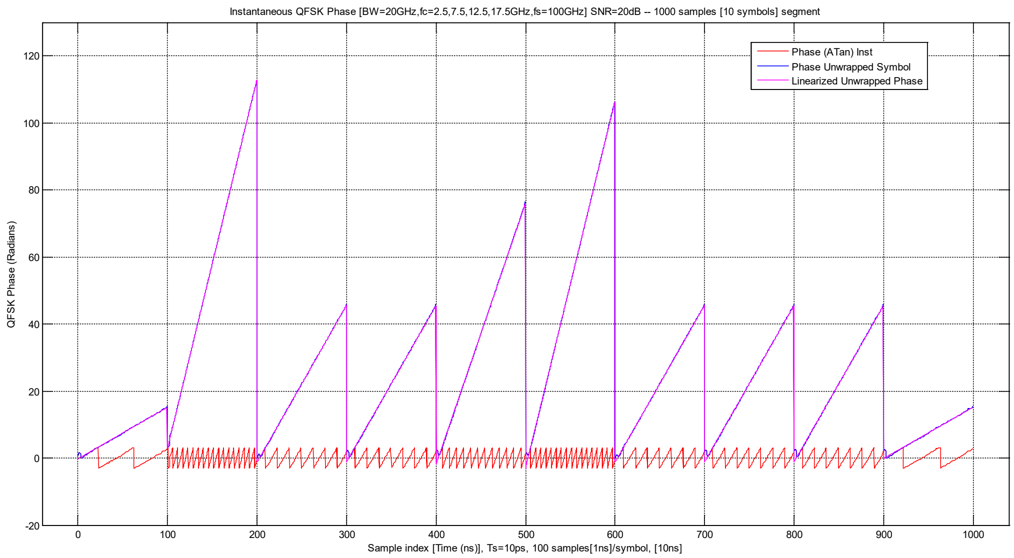

Figure 3.3 Instantaneous and Unwrapped Phase of QFSK

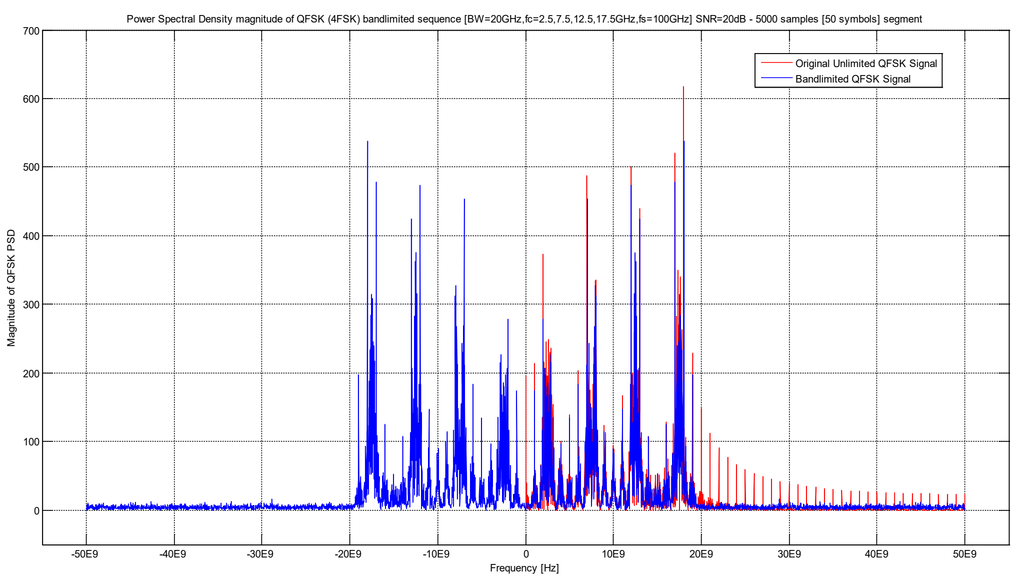

Figure 3.4 Power Spectral Density of QFSK

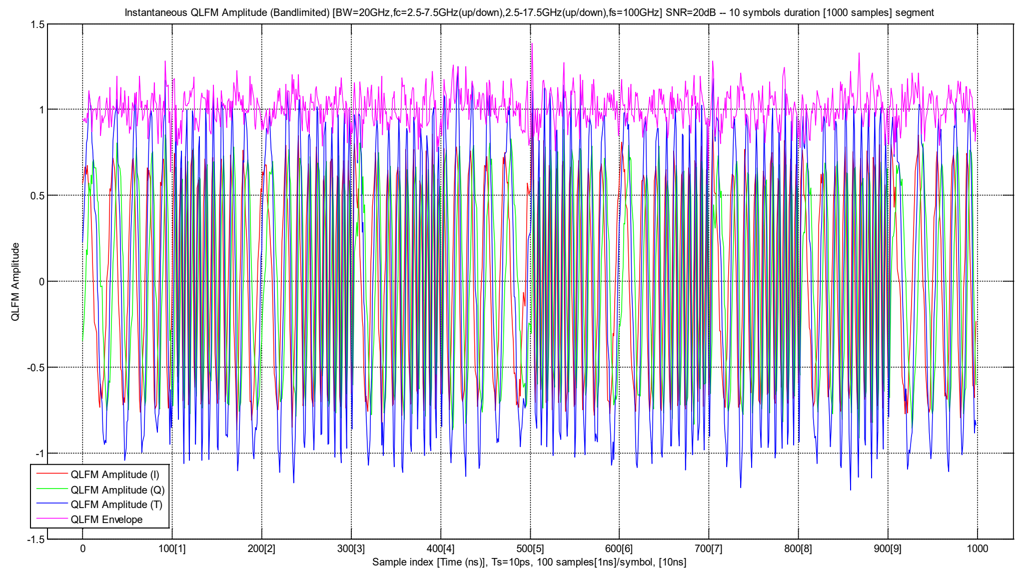

Figure 3.5 Instantaneous Amplitude of QLFM Modulation Format

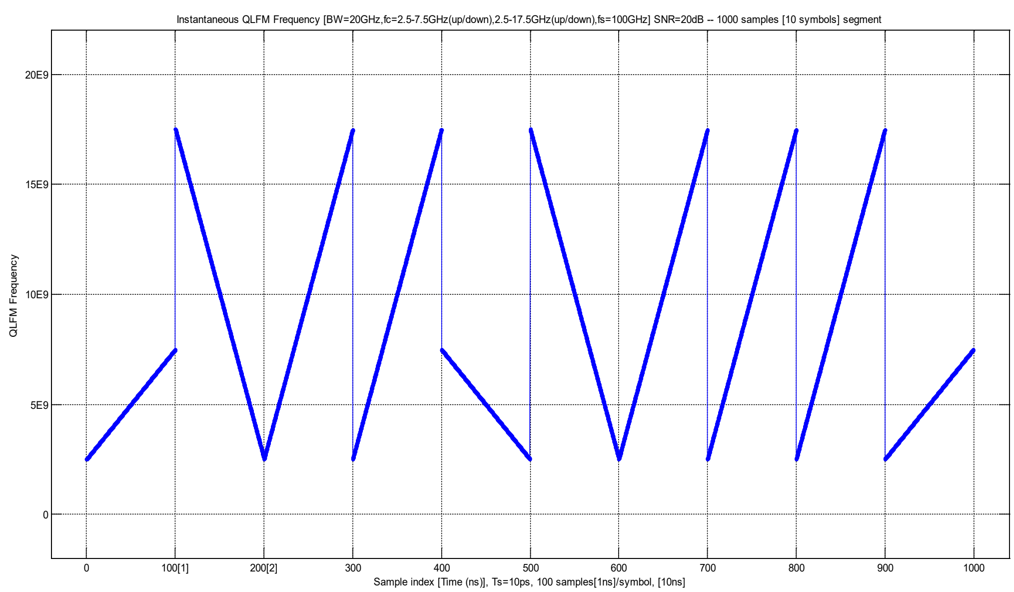

Figure 3.6 Instantaneous Frequency of QLFM Modulation Format

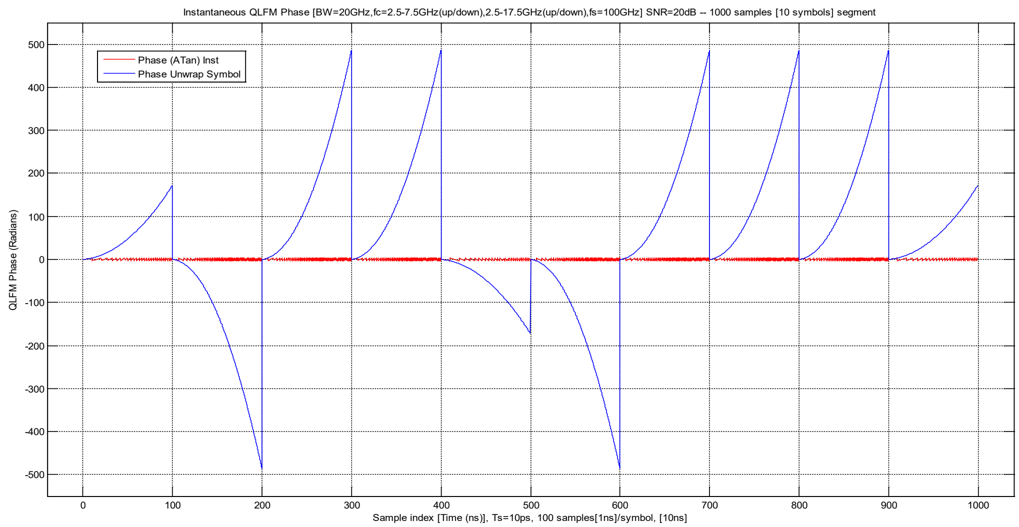

Figure 3.7 Instantaneous and Unwrapped Phase of QLFM

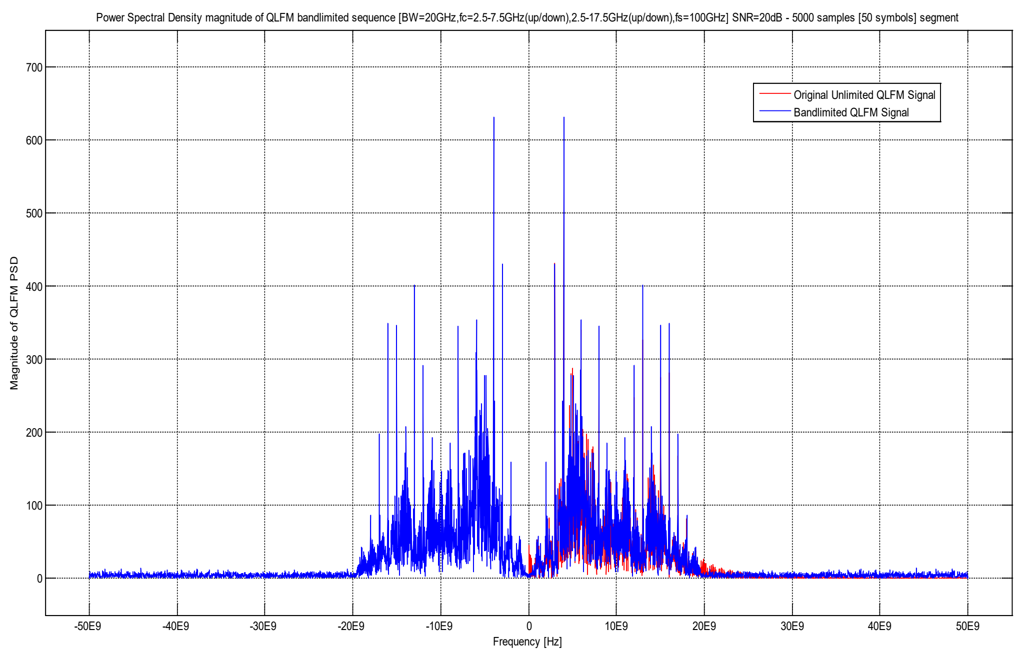

Figure 3.8 Power Spectral Density of QLFM

Sample results for all 8 of the modulation formats that were considered for the SS technique appear in Table 3.2 [22]. The values differ considerably, a good property for potential classification discrimination.

Table 3.2 Listing of Signal Statistics (SS) Features for 20 dB Modulated Waveforms Majority-Selection-Rule Classifier

Signal Statistics	Modulation Type							
	QASK	QFSK	QPSK	QAM44	GMSK	QLFM	QPWM	QPPM
σ_{da}	0.1974	0.0647	0.0918	0.1791	0.1827	0.0481	0.2292	0.2623
σ_{aa}	0.1064	0.0446	0.0701	0.0722	0.0983	0.0289	0.1048	0.1438
μ_{42}^{a}	1.1563	1.0153	1.0280	1.1204	1.1342	1.0092	1.1585	1.3235
σ_{af}	0.0039	2.1202	0.0085	0.0349	0.0080	1.9045	1.5226	1.7295
μ_{42}^{f}	1.0000	1.4856	1.0000	1.0003	1.0001	1.5365	1.4159	1.4573
σ_{dp}	1.8137	1.8024	1.8142	1.8207	1.8710	1.8106	1.5176	0.8660
σ_{ap}	0.9071	0.9012	0.9066	0.9237	1.0165	0.9061	1.0415	0.7851
σ_{dps}	18.1364	27.6398	18.2613	35.4456	36.2065	179.84	18.0712	3.8992
σ_{aps}	18.1361	27.6390	18.1746	18.1670	18.2135	130.48	18.0711	3.8992
$\gamma_{\max}$	1800.9	538.274	659.008	879.776	1191.4	630.9329	1802.2	422.2807
P_{total_norm}	6.1118	164.755	44.118	21.8317	37.8511	89.4911	10.2471	34.7293

3.3.2 Multifractal Features Technique (MF)

Figure 3.9 shows sample curves utilized in determination of the Fractal Dimensions D_6 in the Multifractal technique (MF) [32]. In particular, for the case of BPSK modulation format, D_6 is determined as follows from the middle linear part of the curve:

$$D_6 = \frac{\Delta ln\big(C(6,r)\big)}{\Delta \ln (r)} = \frac{-0.528-(-2.112)}{0-(-1.911)} = 0.829 \tag{32}$$

The authors have modified the multifractal feature vectors slightly to give them greater discrimination capability by spreading the multifractal set from $D_2, D_3, D_4, D_5, D_{6,} D_{7,} D_{8,} D_9$ to

$D_2, D_4, D_6, D_8, D_{10,} D_{12,} D_{14,} D_{16}$. Thus, in this technique, the feature vectors consisted of 8 elements but more spread out in their values compared to original study in [21].

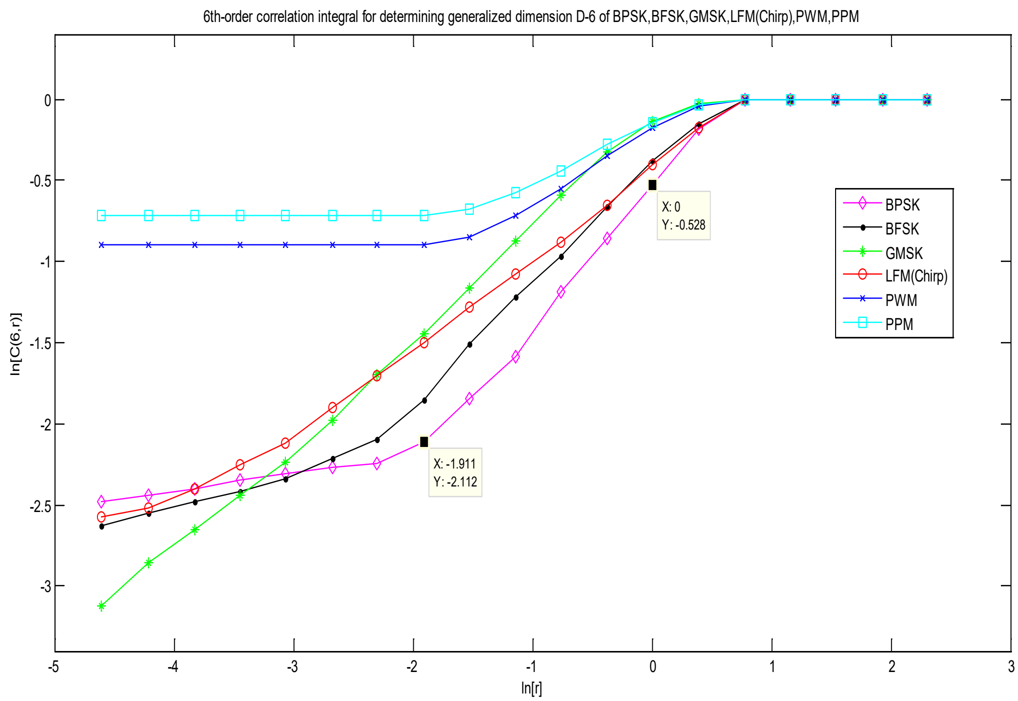

Figure 3.9 Curves for Determination of Fractal Dimension D_6 .

The 3 techniques considered further were Higher Order Statistics – Cumulants (CM), Cyclostationary features (CS) and Fourier Transform of Continuous Wavelet Transform (FWT).

3.3.3 Higher Order Statistics – Cumulants Technique (CM)

A sample 8 element CM feature vector appears in Figure 3.10 and consists of the following cumulants: $C_{20}, C_{40}, C_{60}, C_{80}, C_{100,} C_{120,} C_{140,} C_{160}$.

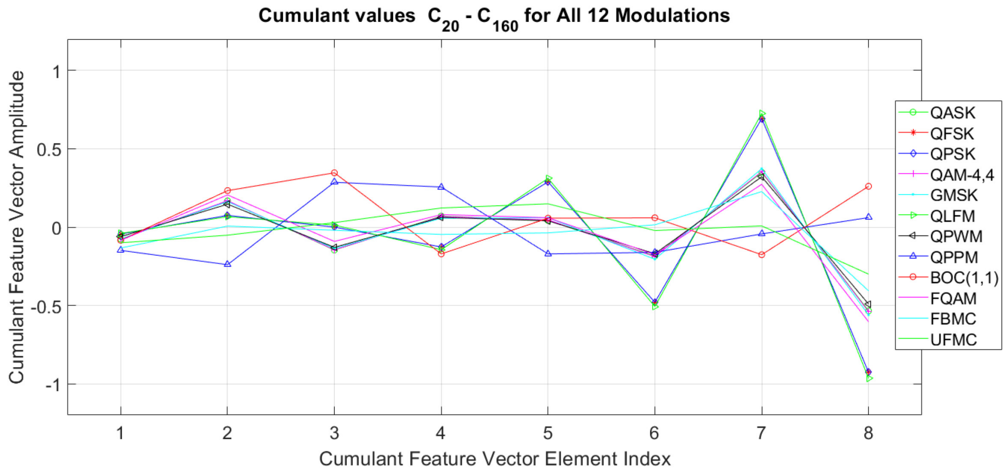

Figure 3.10 Plots of 8 Element Cumulant Feature Vectors

3.3.4 Cyclostationary Features Technique (CS)

Determination of Cyclostationary feature vectors was accomplished in 2 steps: First the Spectral Coherence (SC), which is a 2-D surface obtained by normalizing Spectral Correlation Function (SCF), also known as Spectral Correlation Density (SCD), was calculated utilizing Equation (20a) and then First Principal Component of it was taken by using the Principal Component Analysis (PCA) [33,34]. Figure 3.11 shows a sample SCD surface for QPPM modulation format. Since the Spectral Correlation Density is a 2-D surface the PCA technique is utilized to reduce the dimension to just 1-D vector by selecting the First Principal Component of the original cyclostationary data which is its orthogonal linear transformation to produce the greatest variance (First Eigenvector):

$$w_{(1)} = arg\ max_{\|w=1\|} \left\{ \sum_i \left(x_{(i)} w \right)^2 \right\} \tag{33}$$

Figure 3.12 shows thus obtained First Principal Components for all 12 modulations are shown which are taken as 201 element feature vectors for the classification purpose. Examining these 12 curves, it can be noticed that they are significantly different from one another, a great quality when the goal is using these waveforms for classification of the associated modulation formats.

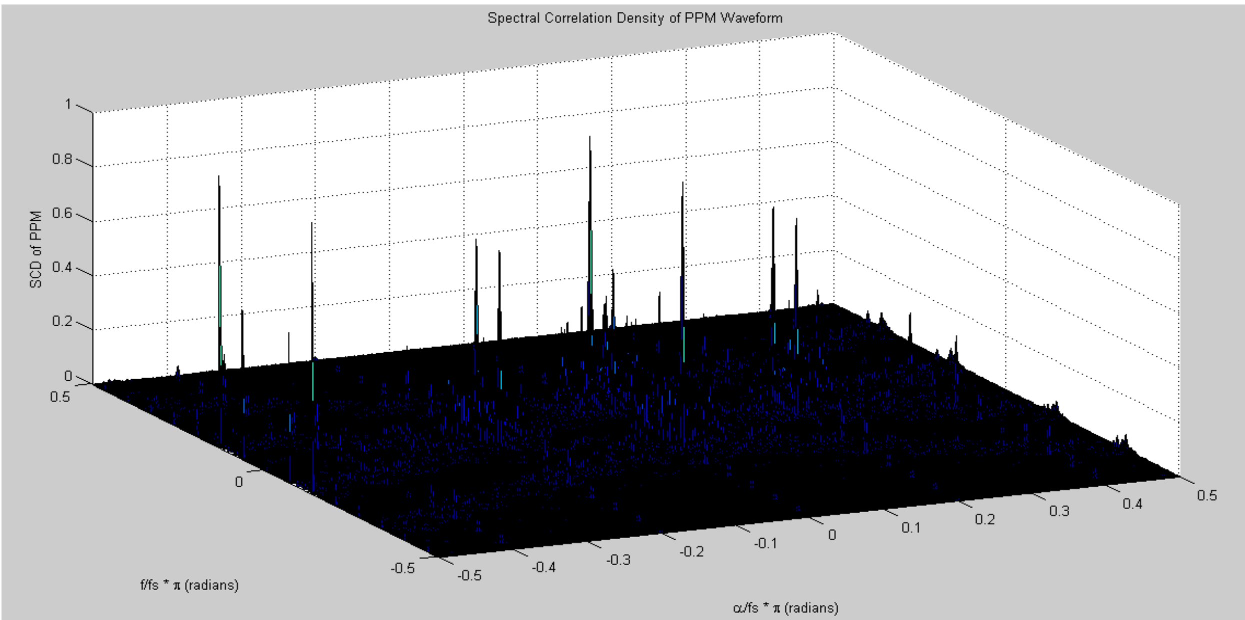

Figure 3.11 Sample SCD Surface for QPPM Modulation Format

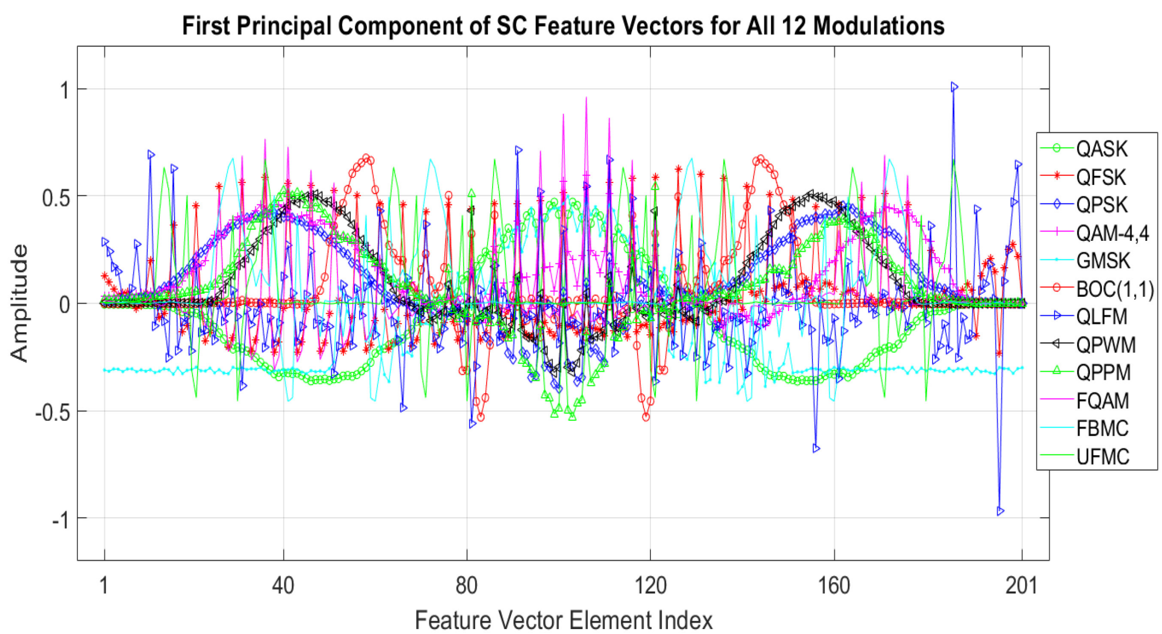

Figure 3.12 First Principal Components for All 12 Modulations

3.3.5 Fourier of Wavelet Transform Technique (FWT)

Finally, the 201 element feature vectors for Fourier Transform of Continuous Wavelet Transform (FWT) technique for all 12 modulation formats are shown in Figures 3.13 and 3.14.

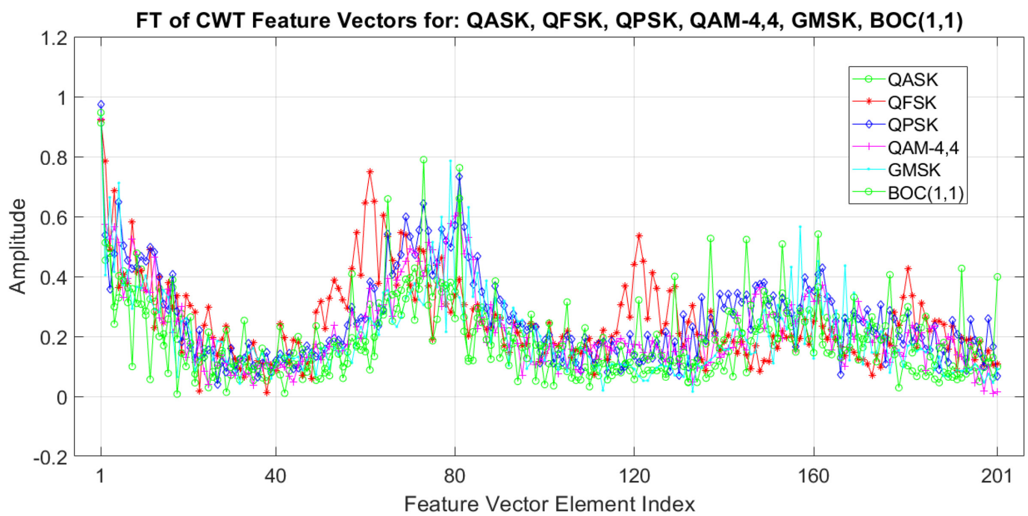

Figure 3.13 Scaled FT of CWT Feature Vectors (First Half)

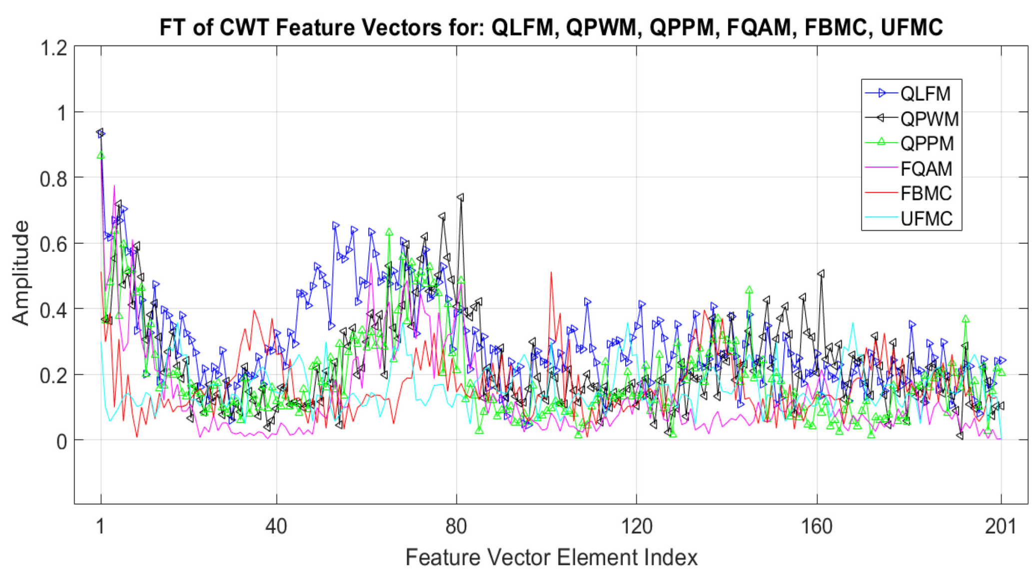

Figure 3.14 Scaled FT of CWT Feature Vectors (Second Half)

3.4 Summary

This chapter described the selection of a large 12-member modulation format set based on literature survey and current commercial and military market status as well as which techniques had the greatest potential for being potentially universally applicable for automatic modulation recognition and source detection. The next chapter will address the aspects of which techniques are best performing and currently most feasible in terms of computational complexity.

Chapter 4: Development of Best Performing and Computationally Feasible Techniques for Near Real-Time Operation

4.1 Selection of Signal Statistics, Higher Order Statistics (Cumulant), Cyclostationary, Multifractal and Fourier of Wavelet Transform Techniques as the Most Widely Applicable for Modulated Signal Recognition

Table 4.1 displays clearly the applicability, complexity, classification performance and noise tolerance for all of the 9 considered feature-based techniques. As can be seen, only the first 5 techniques are considered as potentially universally applicable for identification of various modulation formats while the last 4 are quite limited in coverage and thus were not simulated further. Of the first 5, the SS, CM, CS and MF techniques were identified in the literature survey and the last, FWT, was proposed by the authors of this study.

Table 4.1 Comparison of Feature-Based AMR Techniques

FB Technique	Applicability	Computational Complexity	Performance/ Classification Probability	Noise Tolerance	Comments
Signal Statistics	Universal	Medium	Degrades fairly rapidly with SNR	Degrades with SNR	Needs noise reduction
Higher Order Statistics (Cum.)	Universal	Low	Very Good	Excellent	The best technique overall
Cyclostationary Features	Universal	Medium	Very Good	Excellent	Computation cost considerable
Multifractal Features	Universal	High	Good	Excellent	Can produce too similar features
FT of CWT	Universal	Low	Very Good	Very Good	Another good technique
Wavelet Transform-DWT	Limited: MPSK, MFSK	-	-	-	Not simulated
Constellation Shape	Digital signals only	-	-	-	Not simulated
Zero Crossing	No Amplitude Discrimination	-	-	-	Not simulated
Radon Transform	Only Square or Diamond shaped Constellations	-	-	-	Not simulated

4.2 Narrowing to HOS/Cum (CM), Cyclostationary (CS) and FWT Techniques as the Definitely Best Performing Techniques

As a result of extensive initial simulations of the 5 selected techniques it was learned that two of them, SS and MF, do not perform on par with the expectations. The SS technique had the quite uncorrectable issue of rapid signal features deterioration with noise as the SNR decreased. On the other hand, for the MF technique the computational complexity was about an order of magnitude greater than the next most complex ones, SS and CS. In addition, the MF technique in some cases produced feature vectors that were too similar to give satisfactory classification probabilities. As a result of these early findings, in subsequent research only the CM, CS and FWT were selected as the preferred techniques. Simulations of classification probability were performed for each of these 3 techniques (CM, CS, FWT) separately, as a Majority Selection Rule classifier utilizing these 3 and also in most recent research 410 element compound feature vectors generated as a concatenation of these 3 separate feature vectors were developed [27]. Figures 4.1 and 4.2 show these compound feature vectors for all 12 modulation formats.

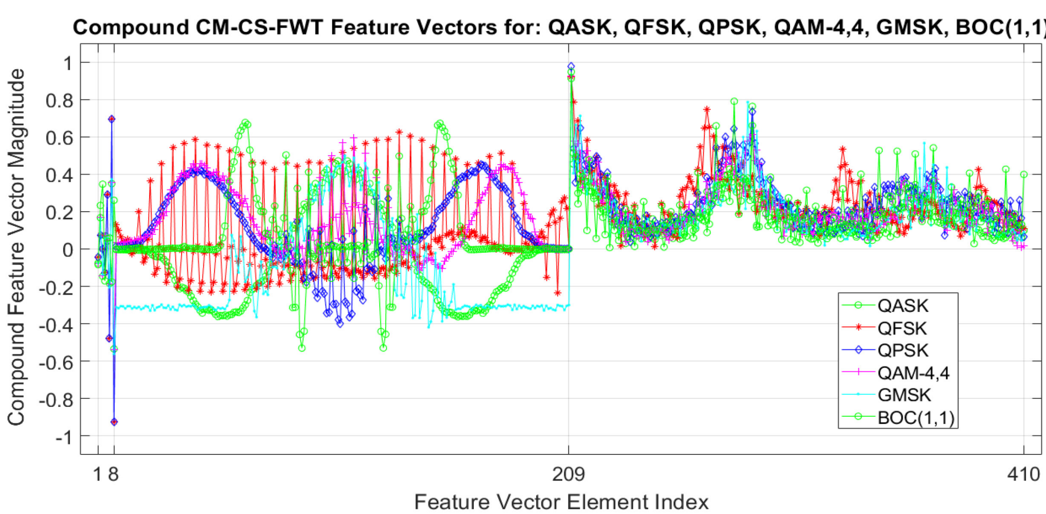

Figure 4.1 Raw Compound 410-Element Feature Vectors (First Half)

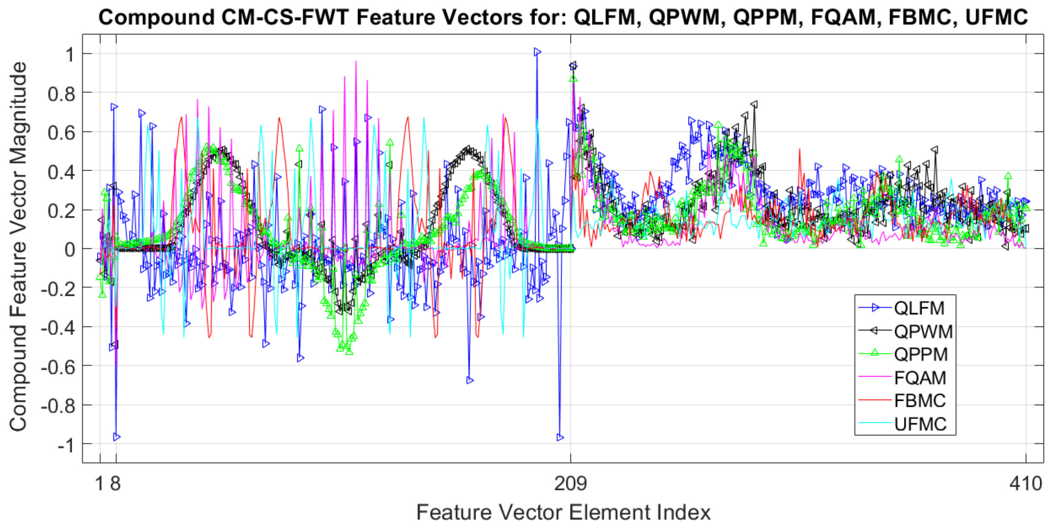

Figure 4.2 Raw Compound 410-Element Feature Vectors (Second Half)

In order to decrease the size of these compound feature vectors and also at the same time increase their discrimination capability, these raw 410 vectors were decreased in size to 90 elements, keeping roughly the same proportion of the 3 feature sub-vectors as in the original sizes (6, 42 and 42), as shown in Figure 4.3.

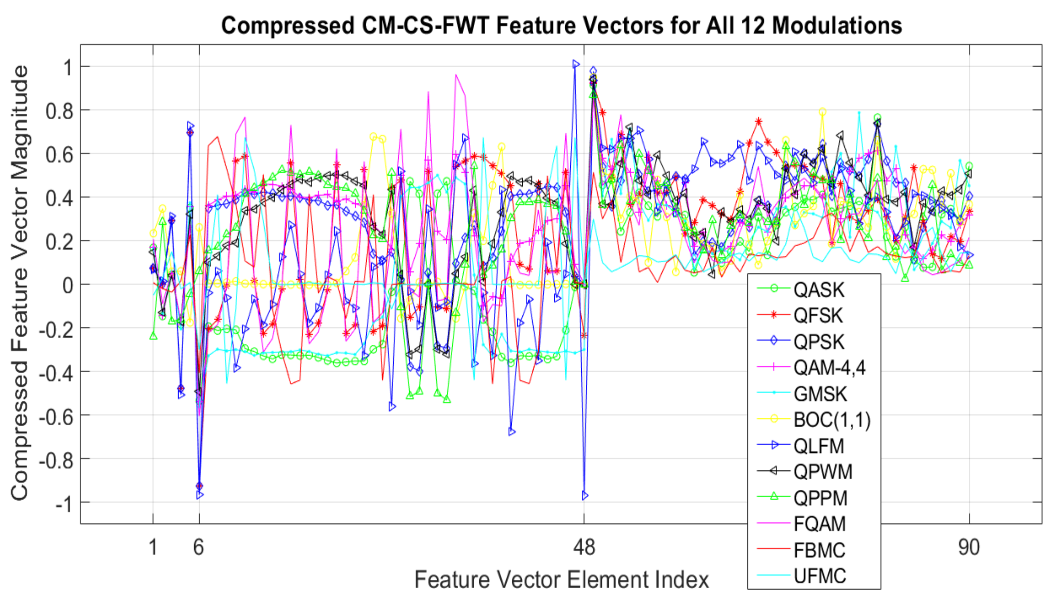

Figure 4.3 Compressed Compound 90-Element Feature Vectors for All 12 Modulations

This size compression was accomplished with the help of variance data compression algorithm as shown in Figure 4.4 where an appropriate threshold for the variance across all modulated waveforms feature vectors is set in order to obtain the desired number of elements [35,36]. The general equation for variance is as follows:

$$Var(X) = \frac{1}{N}\sum_{k=1}^{N}(x_k - \mu)^2 \qquad \mu = \frac{1}{N}\sum_{k=1}^{N} x_k \tag{34}$$

Elements within each of the sub-vectors with variance higher than the determined threshold were kept in the compressed compound vectors.

The optimal compressed size of the compound vectors was experimentally determined to be about 90 elements, so that the probability of correct classification (Pcc) has not changed much from the one for the uncompressed vectors as seen in Figure 4.5.

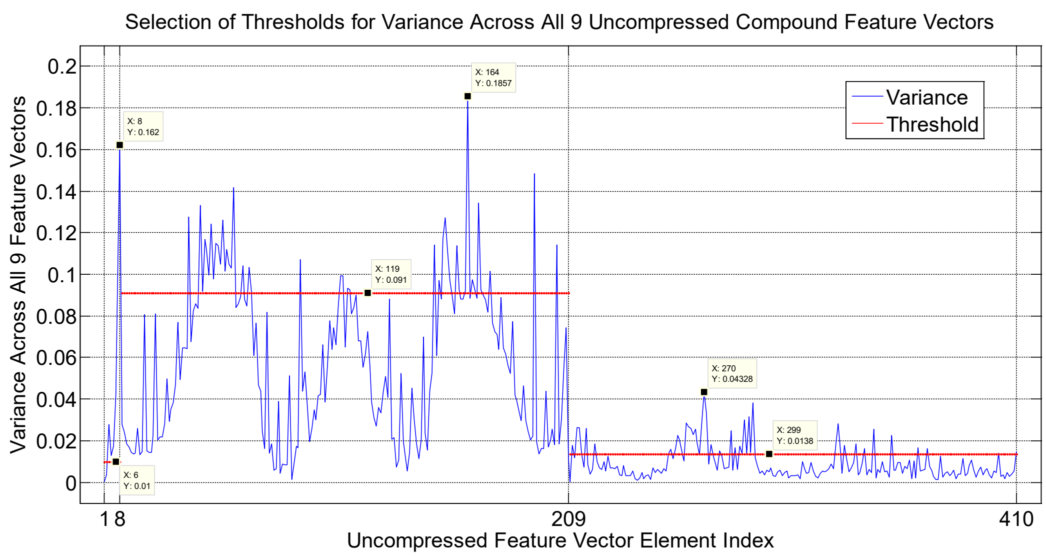

Figure 4.4 Selection of Variance Thresholds across All Modulation Formats in the Test Set

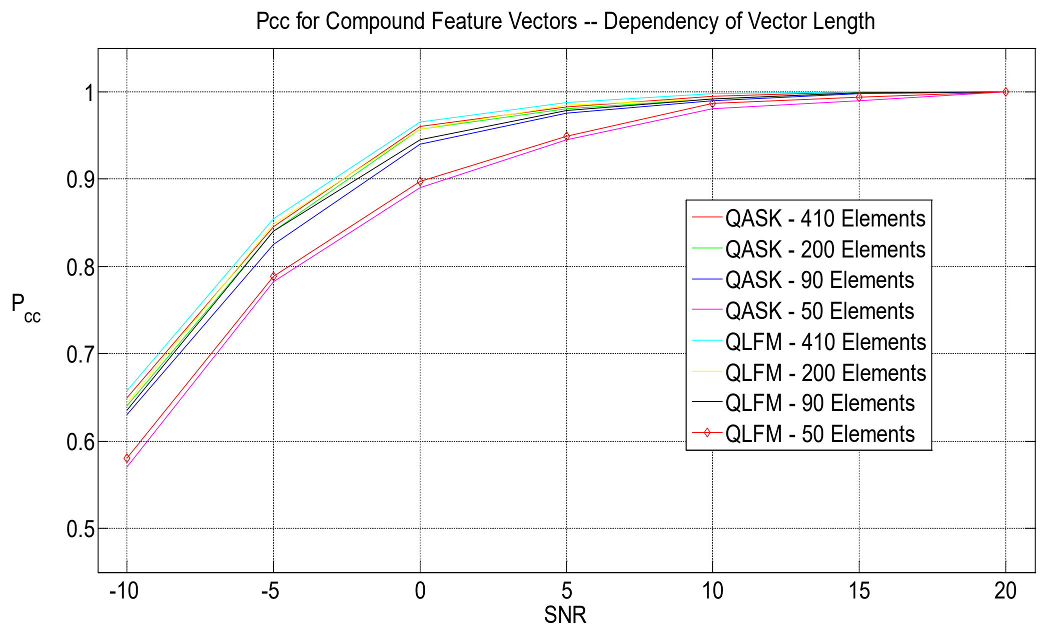

Figure 4.5 Pcc vs. SNR for QASK & QLFM as Function of Vector Length

4.3 Performance of Majority Selection Rule Classifier for Individual CM, CS and FWT Techniques

In the results for the best CM, CS and FWT techniques, 3 experimental setups have been followed as shown in Figure 4.6. The first were single CM, CS and FWT feature vectors classified independently. The second was a Majority-Selection-Rule classifier utilizing single CM, CS and FWT feature vectors. Finally, the third was a distributed multi-receiver classifier making use of the combined CM-CS-FWT feature vectors.

For each of the setups, 100 feature vectors (single or combined) at varying levels of SNR ranging between -10 dB and +20 dB have been used in Neural Network Training and additional 1000 such vectors were utilized in the Testing phase to calculate the resulting probabilities of correct classification (Pcc). All modulated waveforms used in the generation of feature vectors were 1000 symbols in length. For single carrier modulation formats, the carrier frequency of the modulated waveforms was 10 GHz and for multi-carrier and frequency sweeps the frequencies utilized were 2.5, 7.5, 12.5 and 17.5 GHz.

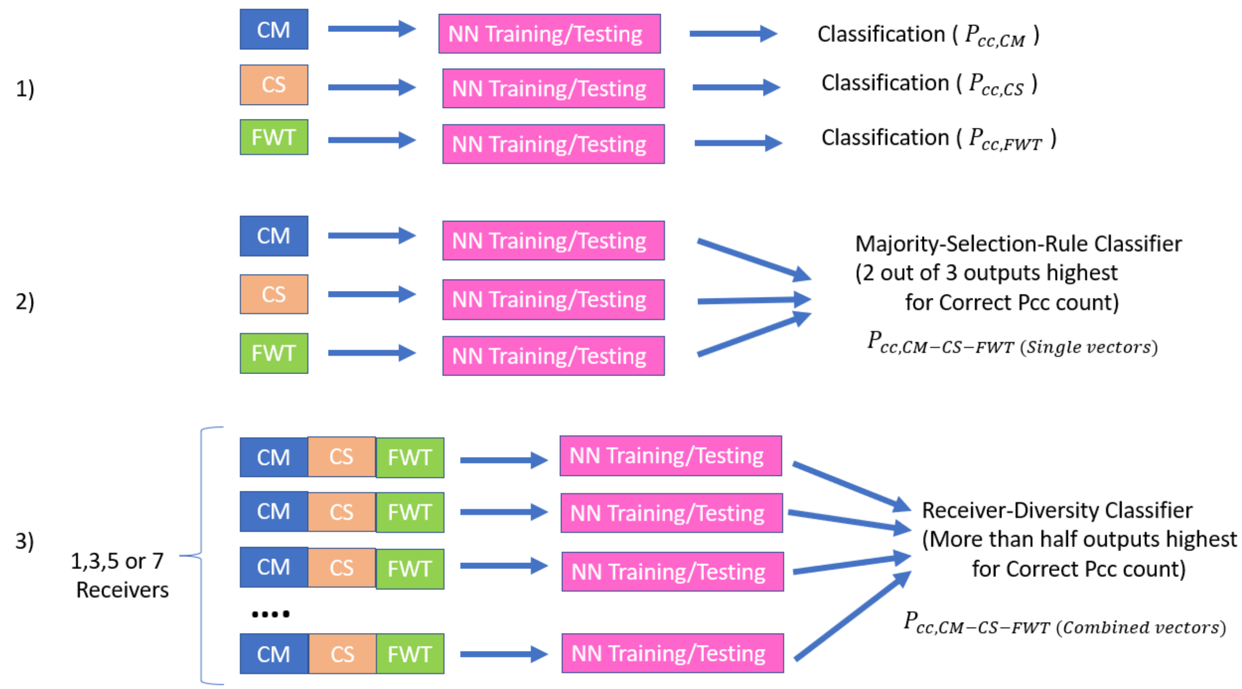

Figure 4.6 Experimental Setups for Analyzing Performance of CM, CS and FWT Feature Vectors

Sample plots of Pcc for the 3 experimental setups for QASK and QLFM modulation formats are shown in Figure 4.7. As can be seen performance of the Majority-Selection Rule classifier utilizing the 3 best feature-based techniques (CM, CS and FWT) is better than the individual techniques performances by about several percent and that for the compound vectors higher still, with the lowest performance for the stand-alone CM technique.

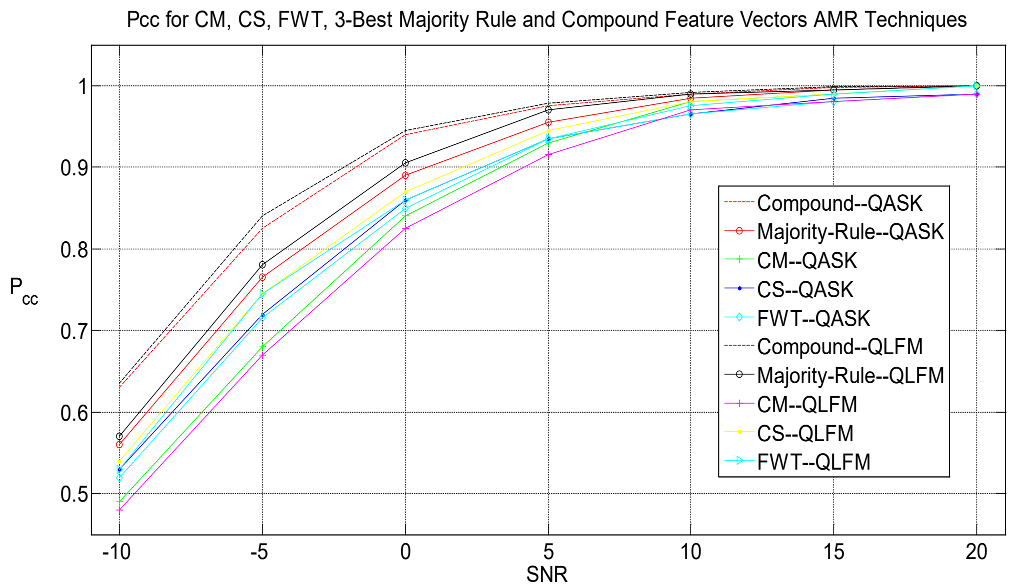

Figure 4.7 Pcc vs. SNR (dB) for 3 Setups [QASK & QLFM]

4.4 Performance of Compound CM / CS / FWT Feature Vector Technique

Plots of Probability of correct classification for several modulation formats comparing performance of combined feature vectors with Majority-Selection Rule classifier utilizing the 3 best feature-based techniques are shown in Figure 4.8. As can be observed the improvement of the compound feature vectors is about 4-5 percent.

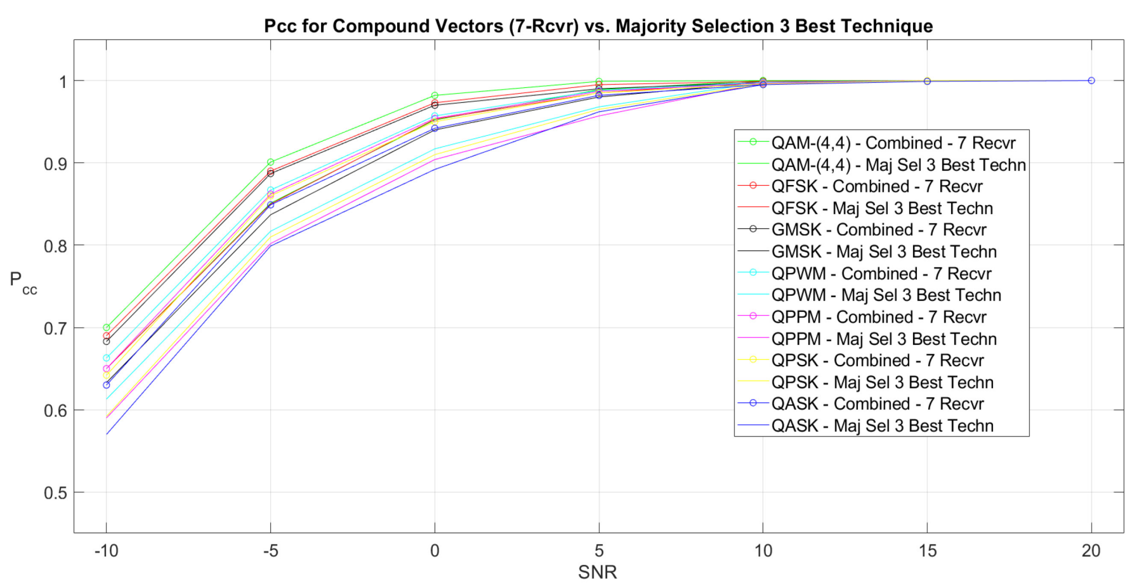

Figure 4.8 Performance of Combined Feature Vectors vs. Majority-Selection Rule Classifier

4.5 Distributed Case up to 7 Receivers for Compound Vector Technique

Plots of Probability of correct classification as a function of the number of receivers in a distributed setup are shown in Figure 4.9 [37,38]. The improvement in performance between no diversity (Single receiver) and 7 receivers is about 6-7 percent.

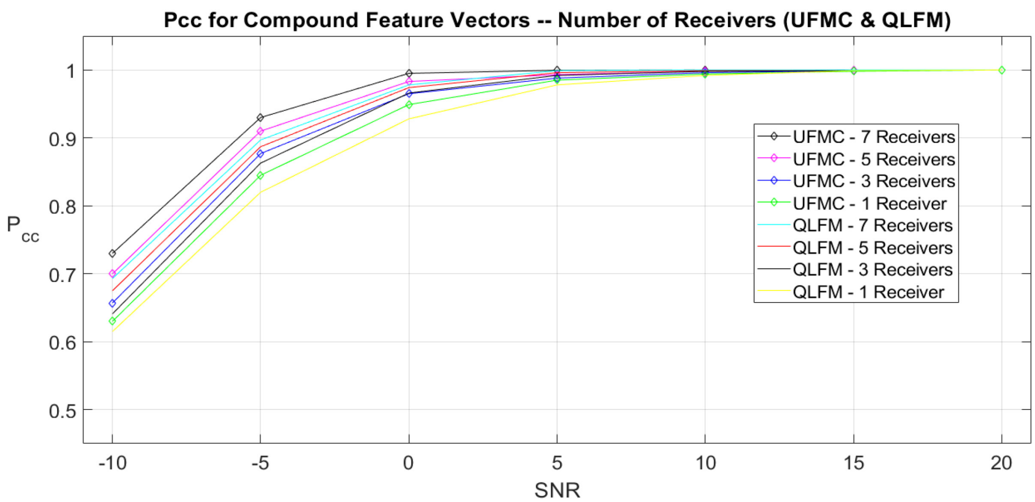

Figure 4.9 Performance as a Function of Number of Receivers (Diversity)

4.6 Summary

This chapter confirmed that the 3 best-performing feature-based techniques CM, CS and FWT selected from among the 5 potentially universally applicable techniques (SS, CM, CS, MF and FWT) had good performance achieving high probabilities of correct classification values for most of the SNR range. The same could not be said about the SS technique whose performance degraded terribly for low SNR values. In the case of MF technique, the performance was also good but it required a considerably longer simulation time to achieve, in some runs more than an order of magnitude longer than the next most complex CS technique. Most notably adding any kind of diversity improves the performance whether it be of the same type (Multiple identical receivers) or varied type (Different feature vectors although for the same modulation format).

Chapter 5: Neural Network (NN) Training and Classification for Evaluation of Proposed AMR Techniques

5.1 Selection of Classification Method for Assessing the Performance of Proposed AMR Techniques

Assessment of the performance, that is pattern recognition classification, of the proposed AMR techniques was implemented with the help of a MaxNet Neural Network structure similar to that in [19] utilizing 12 separate feed-forward back-propagation multilayer linear perceptron networks (FF BP MLPN) processing 100 & 1000 sample feature vectors *x(k), k* = 8, 90 or 201, for training and testing, respectively, for each of the 12 modulation formats and SNR levels as shown in Figure 5.1. The internal structure of each FF BP MLPN is shown in Figures 5.2 and 5.3, where the first figure shows the case of NN Training in order to obtain the necessary weights between the 3 layers using the generated feature vectors and the second of NN Testing, a special case of the first setup, where there is only one output from the NN, $y_\rho, \rho = 1,2,\dots,12$ for each of the modulation formats separately.

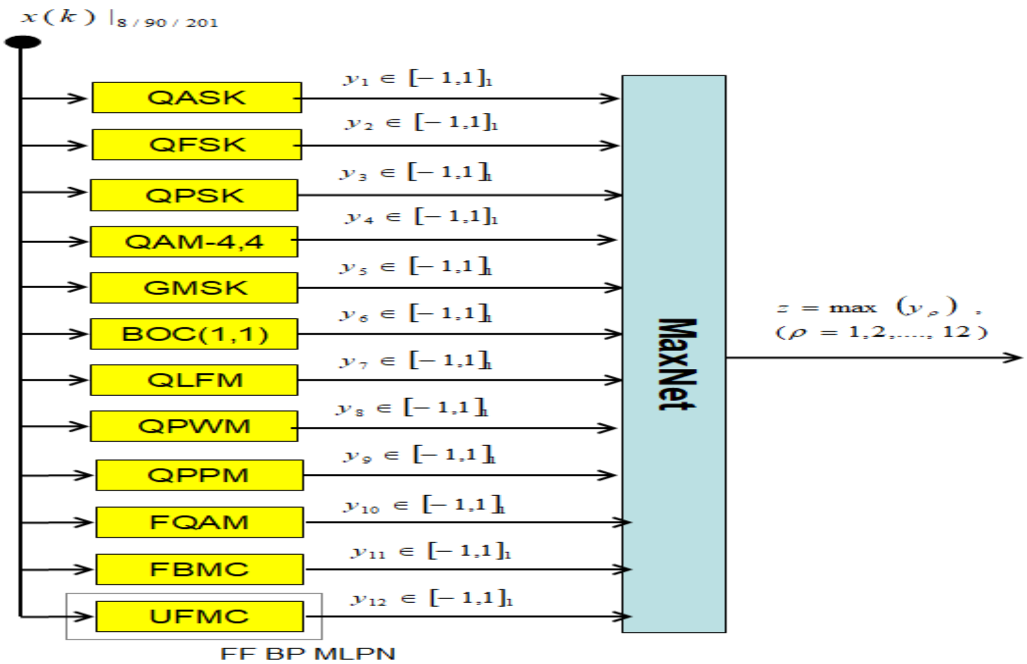

Figure 5.1 MaxNet Structure Used in Neural Network Feature Vector Testing

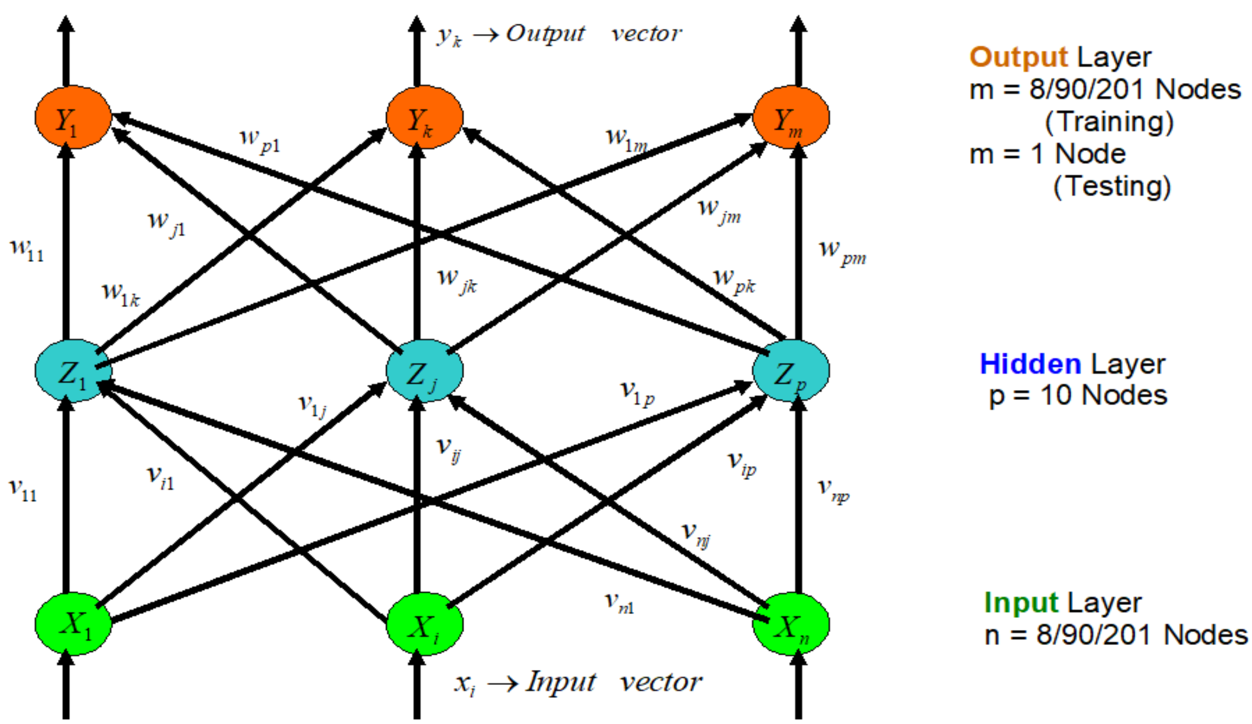

Figure 5.2 The Internal Structure of Each FF BP MLPN Used for Training

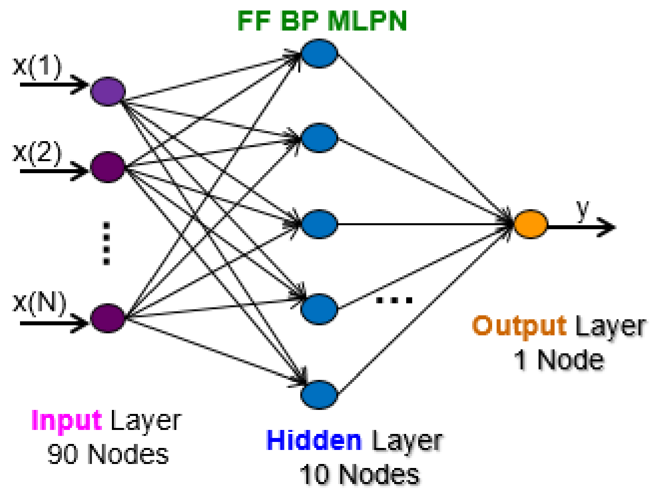

Figure 5.3 The Internal Structure of Each FF BP MLPN Used for NN Testing

5.2 NN Training Using Generated Modulation Format Patterns

The training algorithm for the NN structure of the MaxNet is as shown in Figure 5.4 [39]. In this stage, the Feed-Forward and Back-Propagation operations take place whereby the training weights v_{ij} and w_{jk} between the Input layer and Hidden layer and Hidden layer and Output layer are generated for the training vectors for all 3 techniques (CM, CS and FWT) and all 12 modulation formats. Examples of the weights for the simplest CM Technique that has the shortest xi=8 element feature vectors and thus easiest to visualize are shown in Figures 5.5 – 5.8 for the QPPM and QFSK modulation formats. The other two techniques CS and FWT have 201 element feature vectors in the raw and uncompressed case (Otherwise 42 elements as part of the 90-element combined compressed feature vectors). As can be seen from these figures the weights vary depending on the modulation format in order to adapt to the feature vector's waveform pattern. In addition, some of the modulation formats were faster in converging their training weights, required less iterations, than others. For some 20 iterations were sufficient while others needed even close to 100 to be converged for certain.

Training $n = m = 8 \;\; 11 \;\; or \;\; 201, \quad p = 10,$ [Decreasing each epoch] $\alpha = 0.0500 : 0.0005 : 0.0005, \quad \mu = 0.7$

Initialize weights to random numbers in interval [-0.5, 0.5] ➔ v_{ij} & w_{jk}
While Stopping Condition [# Epochs = 100] is False :
For each **Training Pair**, do Steps 1–6 :
[Feed-forward]

Step 1 -- Each Input Node Xi (i=1:n), receives input signal xi and broadcasts it to all units in hidden layer above

Step 2 -- Each Hidden Node Zj (j=1:p), sums its weighted input signals:

$$z\_in_j = \sum_{i=1}^{n} x_i \cdot v_{ij}$$

Applies its activation function to compute its output signal:

$$z_j = \tanh(z\_in_j)$$

And sends this signal to the nodes in output layer above.

Step 3 -- Each Output Node Yk (k=1:m) sums its weighted input signals:

$$y\_in_k = \sum_{j=1}^{p} z_j \cdot w_{jk}$$

And applies its activation function to compute its output signal:

$$y_k = \tanh(y\_in_k)$$

[Back-propagation of error]
Step 4 -- Each Output Node Yk (k=1:m) receives a target pattern (*tp*) corresponding to input training pattern,
Computes its error information term by multiplying the difference by derivative of activation function :

$$\delta_k = (tp_k - y_k)[(1 + \tanh(y\_in_k))(1 - \tanh(y\_in_k))]$$

Calculates its weight correction term:

$$\Delta w_{jk} = \alpha \delta_k z_j \quad \text{or} \quad \Delta w_{jk}(t+1) = \alpha \cdot \delta_k z_j + \mu \cdot \Delta w_{jk}(t)$$

And sends δ_k to nodes in layer below (Hidden Nodes)

Step 5 -- Each Hidden Node Zj (j=1:p) sums its delta inputs from nodes in output layer above:

$$\delta\_in_j = \sum_{k=1}^{m} \delta_k \cdot w_{jk}$$

Multiplies by derivative of its activation function to calculate its error information term:

$$\delta_j = \delta\_in_j \{(1 + \tanh(z\_in_j))(1 - \tanh(z\_in_j))\}$$

And calculates its weight correction term:

$$\Delta v_{ij} = \alpha \delta_j x_i \quad \text{or} \quad \Delta v_{ij}(t+1) = \alpha \cdot \delta_j x_i + \mu \cdot \Delta v_{ij}(t)$$

[Update Weights]
Step 6 – Each Output Node Yk (k=1:m) updates its weights:

$$w_{jk}(new) = w_{jk}(old) + \Delta w_{jk}$$

And each Hidden Node Zj (j=1:p) updates its weights:

$$v_{ij}(new) = v_{ij}(old) + \Delta v_{ij}$$

Test Stopping Condition

Figure 5.4 Training Algorithm for the NN Structure of the MaxNet

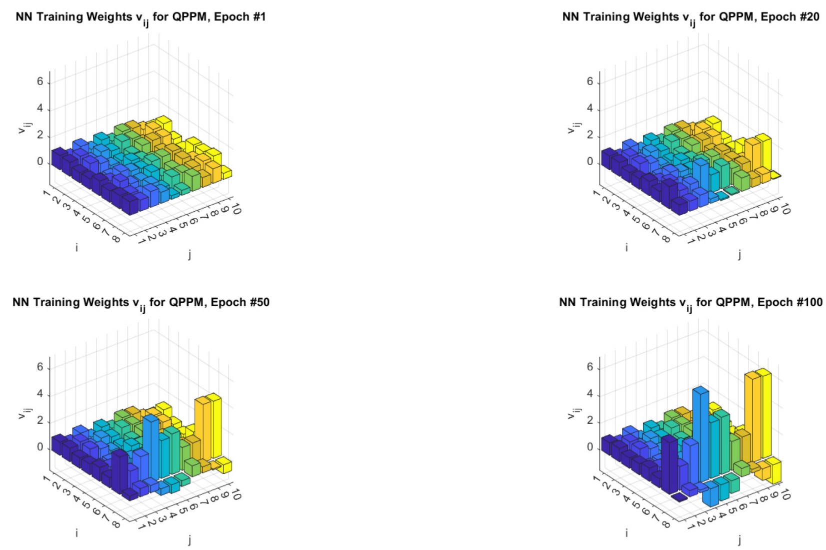

Figure 5.5 Neural Network Training Weights v_{ij} Calculated from QPPM Cumulants Feature Vectors Showing the Progression Through Multiple Iterations (Epochs)

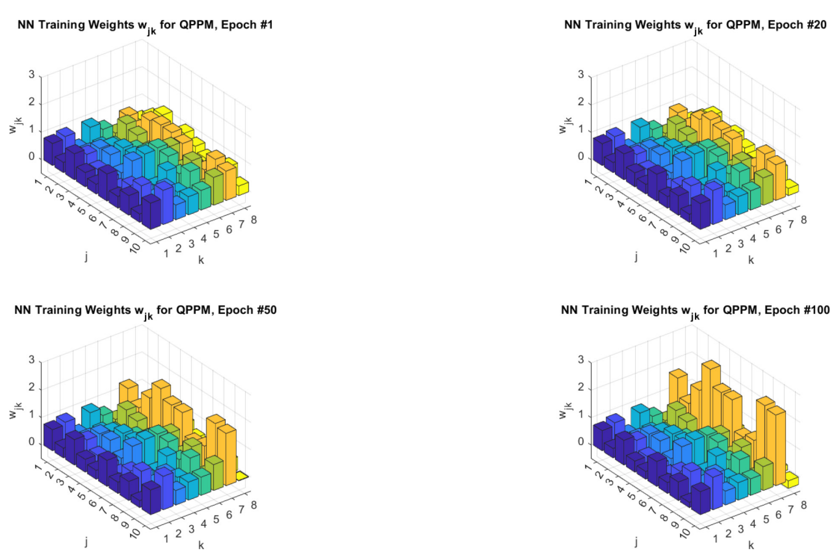

Figure 5.6 Neural Network Training Weights w_{jk} Calculated from QPPM Cumulants Feature Vectors

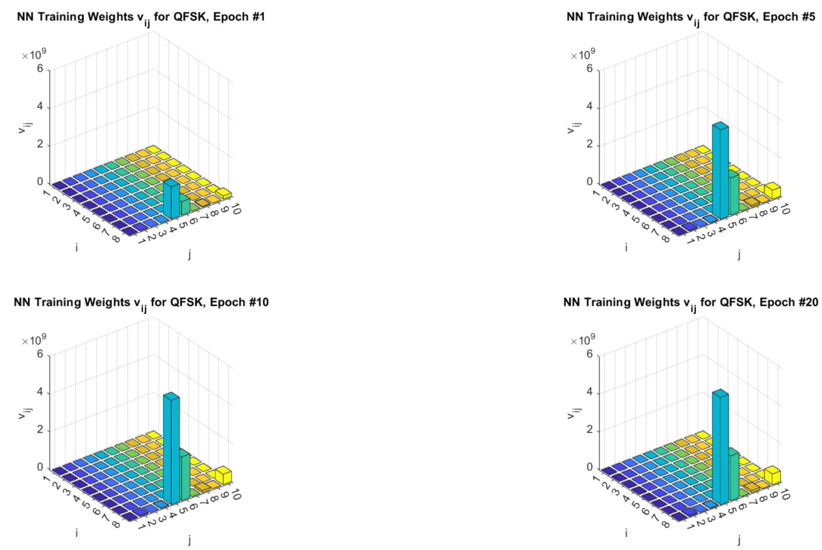

Figure 5.7 Neural Network Training Weights v_{ij} Calculated from QFSK Cumulants Feature Vectors

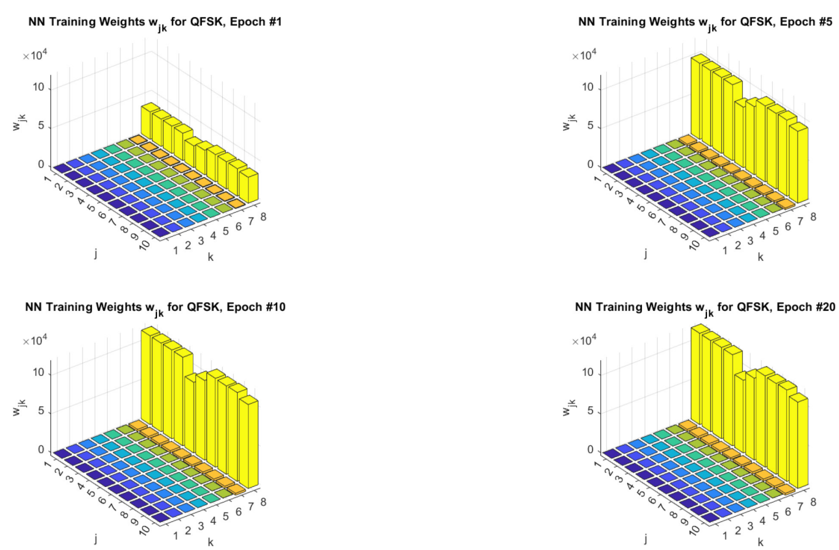

Figure 5.8 Neural Network Training Weights w_{jk} Calculated from QFSK Cumulants Feature Vectors

5.3 NN Classification Utilizing Previously Stored Feature Vectors

To calculate the Probabilities of correct classification Pcc for each of the modulation formats by using the weights generated by the Training Algorithm, only the Feed-Forward phase of NN algorithm shown in Figure 5.9 is used as in Figure 5.10.

Initialize weights from the Training Algorithm
For each Input Vector, do Steps 1-3 :

Step 1 – For i = 1 : n, set activations of Input Nodes x_i

Step 2 – For j = 1 : p,

$$z\_in_j = \sum_{i=1}^{n} x_i \cdot v_{ij} \;\rightarrow\; z_j = \tanh(z\_in_j)$$

Step 3 – For k = 1 : m (= 1),

$$y\_in_1 = \sum_{j=1}^{p} z_j \cdot w_{j1} \;\rightarrow\; y_1 = \tanh(y\_in_1)$$

Figure 5.9 NN Application Algorithm Used to Calculate Pcc for All Modulation Formats

Figure 5.10 illustrates the calculation of probability of correct classification (Pcc) for UFMC modulation format in 3-Receiver Majority-Selection-Rule (Identical type diversity) scheme. For each of the 20 trial runs shown in the figure, there are 12 outputs of the NN obtained by utilizing the application / testing algorithm in Fig. 5.9. Ideally, the highest output should come from the feature vector corresponding to modulation format that produced it. Any errors would be caused by noisy feature vectors, especially at lower SNR values. If the appropriate output is indeed highest that constitutes a correct count towards calculating probability of correct classification Pcc: Number of positive counts divided by total number of trial runs. Fig 5.10 shows just 20 runs for illustrative purpose; however, actually there were 1000 trials used in determination of Pcc.

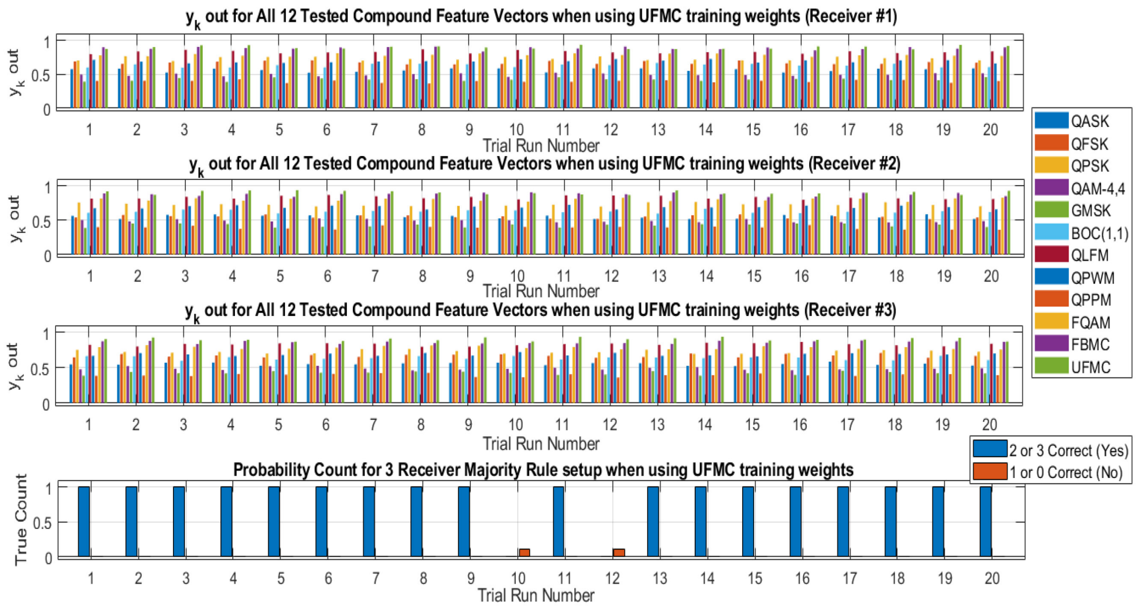

Figure 5.10 Illustration of Probability of Correct Classification (Pcc) Calculation for UFMC Modulation Format

The case pictured is for 3 receivers. In the case of 5 and 7 receivers there were additional 2 and 4 Neural Network output sub-plots for the corresponding receivers. If a minimum of 2 out of 3 Neural Network outputs for the receivers gave the highest result that constituted a true count towards the Pcc calculation. For 5 receivers that was 3 out of 5 and for 7 receivers, 4 out of 7 [37,38].

5.4 Summary

The MaxNet Neural Network structure is a convenient way to perform the Neural Network training to obtain the weights which are subsequently utilized in the determination of Probabilities of correct classification for all 12 modulation formats. Usually 100 Epochs (Loops of the training algorithm) were sufficient to generate sufficient weights for the modulation format pattern recognition. Some feature vectors were quicker than others to reach training convergence.

Chapter 6: Comparison of the AMR Classification Performance of Proposed Techniques with the Results in the Literature

6.1 Modulation Format Coverage and Sizes of Evaluation Test Sets of Current Techniques

As mentioned in Chapter 3, the authors of this study have gathered one of the largest and most varied up do date modulation format test sets in the literature on this subject of AMR in comparison with the survey results in Table 3.1.

6.2 Performance of the Proposed Technique Versus the Already Existing Ones

There is not much in the current literature to compare this study with directly since most likely nobody has considered such a comprehensive modulation format test set. In addition, quite many of the proposed techniques were describing awkward and inconvenient to implement in practice hierarchical classification schemes [8,9,13,15]. For example, in [13] there is one of such hierarchical setups. First, it utilizes Cumulant C42 to discriminate between 8,32-QAMstar, 16,64-QAMstar, MQAM, BPSK, PSK (n>2) and ASK (n>2) and then again Cumulant C42 and C80 to fine tune the classification into appropriate modulation order. This is still, however, quite small and not very varied modulation format set. As can be seen in the performance comparison of this technique with the one proposed by the authors for compound feature vectors with 7 receiver diversity in Figure 6.1 the results are dramatic. The explanation for this performance discrepancy is the size of the feature vectors used in the classification, 1 vs. 90 applied 7 times and variance maximized for additional discrimination capability.

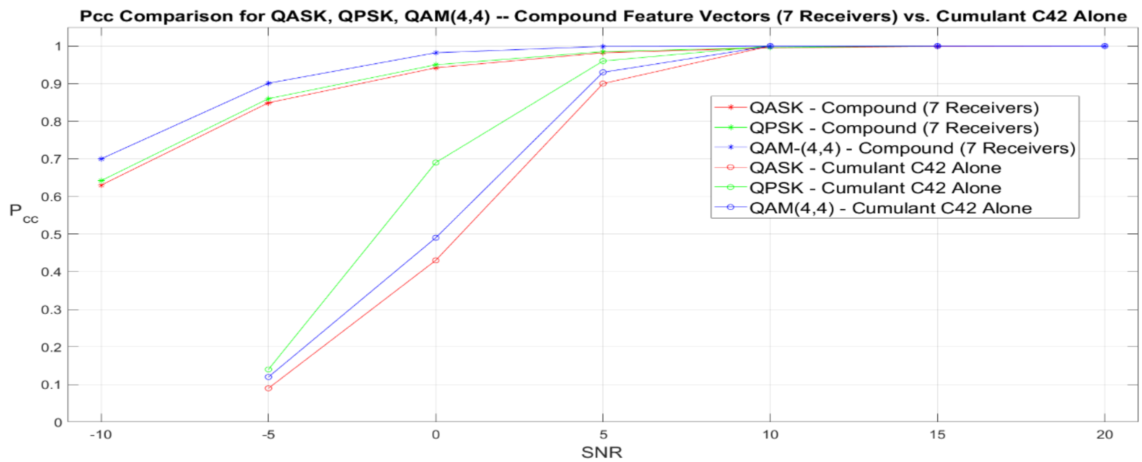

Figure 6.1 Comparison of Pcc vs. SNR for QASK, QPSK and QAM(4,4) Modulation Formats for Latest Combined Feature Vectors vs. Cumulant C42 Alone

6.3 Summary

Looking at the potential applicability of the demonstrated 3 best feature-based technique scheme utilizing compound feature vectors and receiver diversity, it is quite certain it will find its way in some form to the newly developed DoD ABMS system and VDATS TPS Development as well as many numerous communications applications as the possibilities are essentially endless. The scheme proposed in this study avoids the multi-level hierarchical classification employed by some of the authors in the earlier research on AMR. There are communication signals everywhere and the need to recognize what they are is necessary for implementing many tasks and missions.

Chapter 7: Conclusion and Future Research

7.1 Conclusion

As demonstrated in the previous chapters, the proposed 3 best feature-based AMR techniques (CM, CS and FWT) are very effective in distinguishing a large and varied modulation format set not previously addressed by any single research team to the best of the authors knowledge. These techniques potentially have universal applicability to any conceivable modulation format that has a waveform in the time domain which can then be also transformed to frequency and wavelet domains. As can be observed in Figures 4.6 – 4.8, adding any kind of diversity improves the classification performance over just the individual CM, CS and FWT techniques considered separately, with the several-receiver compound feature vectors performance being about 5% higher than the Majority-Selection-rule setup utilizing 3 individual CM, CS and FWT techniques. This is a significant improvement which is always welcomed.

The research presented in this study examined which feature-based techniques are readily applicable and which should be avoided due to their very limited coverage and gave a convenient and effective non-hierarchical method for modulation format classification with reasonable computational complexity in order to be suitable for real-time implementation. Most certainly some variant of the highest-performing compound feature vector AMR setup with distributed receivers described in this study will have numerous applications in the near future, both commercial and defense, as the communications systems are getting constantly more complicated with an increasing number and variety of modulation formats.

7.2 Future Research

Future research could attempt to address the performance of higher order (M > 16) of modulation techniques employed in FQAM, FBMC and UFMC by utilizing this feature-based AMR technique. In addition, performance in channels other than AWGN, such as Frequency Selective and Impulsive channels, may be studied [40].

The authors also envision possibly adding the Multifractal technique to make the compound feature vectors even larger and possibly further increase their discrimination capability. This would require greater computational complexity though but as the technology advances this may not be an issue soon. Then there is also the possibility of fixing the Signal Statistics technique's performance although creating an effective waveform equalization may not be an easy task.

In addition, there is a possibility of incorporating the Weighted Ensemble Testing scheme in the 2nd and 3rd diversity experimental setups shown in Figure 4.6 whereby the outputs from the Neural Network testing phase are assigned appropriate weights based on its particular capability or efficiency.

In order to speed up the execution of the AMR Technique on the VDATS test station the authors would like to improve the interfaces within the overall VDATS tester setup as shown in Figure 7.1. As can be seen, there are up to six basic interfaces: Between DA unit and computer (1), DA unit and RF unit (2), DA unit and roll-up rack (3) and RF unit and roll-up rack (4) are cables mainly of coaxial type. On the other hand, the interfaces between the DA unit and ITA (5) and ITA and UUT (6) are serial or parallel busses. ITA stands for Interface Test Adapter and UUT is the Unit Under Test.

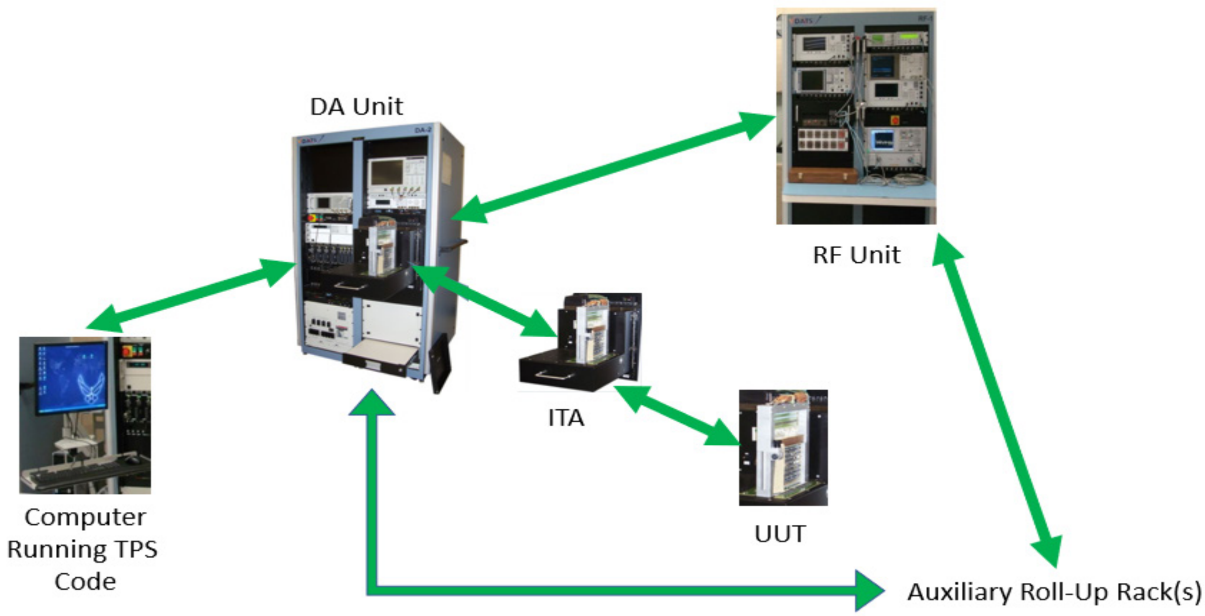

Figure 7.1 Interfaces Schematic Within Overall VDATS Tester Setup

Some of the other methods to increase the speed of TPS execution would be improving the efficiency of the compiled code on the Computer CPU and introduction of other test specific languages. For example, the Automatic Test Markup Language (ATML) defines the interfaces that streamline TPS development. The purpose of ATML is to support test program, test asset and Unit Under Test (UUT) interoperability within an automatic test environment. ATML accomplishes this through a standard medium for exchanging UUT, test and diagnostic information between components of the test system. ATML provides promise for future software standardization; however, it cannot be applied to legacy test systems.

References

[1] K. Osborn, "The Air Force is Creating a System to Manage the Military's Forces in War," *The National Interest*, Mar 2018, https://nationalinterest.org/blog/the-buzz//the-air-force-creating-system- manage-the-militarys-forces-24701?page=0%2C1 .

[2] A. McCullough, "Life After JSTARS," *Air Force Magazine*, Apr 2019, http://www.airforcemag.com/MagazineArchive/Pages/2019/April%202019/Life-After-JSTARS.aspx .

[3] J. Mitola III, "Cognitive Radio for Flexible Mobile Multimedia Communications," *IEEE Workshop on Mobile Multimedia* and *Communications*, pp. 3-10, Nov 1999.

[4] W. L. Adams Jr, "Solving the U.S. Air Force's ATS Proliferation Problem – The VDATS Solution," *Proc. IEEE AutoTestCon,* pp. 598-600, Sep 2008.

[5] Q. Shi and Y. Karasawa, "On Signal Phase Based Modulation Classification," *IEEE Int'l Conference on Communications (ICC)*, pp.1-5, 2011.

[6] J.L. Xu, W. Su and M. Zhou, "Software-Defined Radio Equipped With Rapid Modulation Recognition," *IEEE Trans. Vehicular Technology*, vol. 59, no.4, pp.1659-1667, May 2010.

[7] M. M. Roganovic, A.M. Neskovic and N. Neskovic, "Application of Artificial Neural Networks in Classification of Digital Modulations for Software Defined Radio," *Proc. IEEE EUROCON*, pp. 1700-1706, 2009.

[8] A.K. Nandi and E.E. Azzouz, "Algorithms for Automatic Modulation Recognition of Communication Signals," *IEEE Trans. Communications*, vol.46, no.4, p.431-436, Apr 1998.

[9] E.E. Azzouz and A.K. Nandi, "Automatic Identification of Digital Modulation Types," Signal Processing, vol.47, no.1, pp.55-69, Nov 1995.

[10] W. Su, "Feature Space Analysis of Modulation Classification Using Very High-Order Statistics," IEEE Communications Letters, vol.17, no.9, pp.1688-1691, Sep 2013.

[11] V.D. Orlic and M.L. Dukic, "Automatic Modulation Classification: Sixth-order Cumulant Features as a Solution for Real-world Challenges," *20th Telecommunications Forum (TELFOR)*, PP.392-399, Nov 2012.

[12] M. W. Aslam, Z. Zhu and A.K. Nandi, "Automatic Digital Modulation Classification Using Genetic Programming with K-Nearest Neighbor," *Proc. IEEE MILCOM*, pp.1731-36, 2010.

[13] L. Liu and J. Xu, "A Novel Modulation Classification Method Based on High Order Cumulants," *IEEE Conf. on Wireless Communications, Networking and Mobile Computing (WiCOM)*, pp.1-5, Oct 2006.

[14] O.A. Dobre, Y. Bar-Ness and W. Su, "Higher Order Cyclic Cumulants for High Order Modulation Classification," *Proc. IEEE MILCOM*, pp.112-117, 2003.

[15] A. Swami and B. M. Sadler, "Hierarchical Digital Modulation Classification Using Cumulants," IEEE Trans. Communications, vol.48, no.3. pp.416-429, Mar 2000.

[16] L. Zhou and H. Man, "Distributed Automatic Modulation Classification Based on Cyclic Feature via Compressive Sensing" *Proc. IEEE MILCOM*, pp.40-45, 2013.

[17] W.C. Headley, J.D. Reed and C. da Silva, "Distributed Cyclic Spectrum Feature - Based Modulation Classification," *Proc. IEEE Wireless Communications and Networking Confefrence*, pp.1200-1204, 2008.

[18] K. Kim, I.A. Akbar, K.K. Bae, J.-S. Um, C.M. Spooner and J.H. Reed, "Cyclostationary Approoaches to Signal Detection and Classification in Cognitive Radio," *IEEE DySpAN (Dynamic Spectrum Access Networks)*, pp.212-215, 2007.

[19] A. Fehske, J. Geaddert and J.H. Reed, "A New Approach to Signal Classification Using Spectral Correlation and Neural Networks," *IEEE International Symposium on New Frontiers in Dynamic Spectrum Access Networks,* pp.144-150, Nov 2005.

[20] M. Oner and F. Jondral, "Cyclostationarity Based Air Interface Recognition for Software Radio Systems," *Proc. IEEE Radio and Wireless Conference*, pp.263-266, 2004.

[21] T. He, Z. Zhou and X. Li, "Modulation Classification Based on Multifractal Features," *Proc. Conf. on ITS Telecommunications*, vol.1, pp.152-155, 2006.

[22] S. Sobolewski, W. L. Adams Jr and R. Sankar, "Universal Nonhierarchical Automatic Modulation Recognition Techniques For Distinguishing Bandpass Modulated Waveforms Based On Signal Statistics, Cumulant, Cyclostationary, Multifractal And Fourier-Wavelet Transforms Features," *Proc. IEEE MILCOM*, pp.748-753, Oct 2014.

[23] K.C. Ho, w. Prokopiw and Y.T. Chan, "Modulation Identification of Digital Signals by the Wavelet Transform," *Proc. IEE Radar, Sonar and Navigation*, vol.147, no.4, pp.169-177, Aug 2000.

[24] B.G. Mobasseri, "Constellation Shape as a Robust Signature for Digital Modulation Recognition," *Proc. IEEE MILCOM*, pp.442-446, 1999.

[25] S.-Z. Hsue and S.S. Soliman, "Automatic Modulation Classification Using Zero Crossing," *Proc. IEE Part F Radar & Signal Processing*, vol.137, no.6, pp.459-464, Dec 1990.

[26] S.L. Wood, M.J. Ready and J.R. Treichler, "Constellation Identification Using the Radon Transform," *Proc. ICASSP*, pp.1878-1881, 1988.

[27] S. Sobolewski, W. L. Adams Jr and R. Sankar, "Effective and Efficient Compound Feature Vectors Applicable To Discrimination Of Any Conceivable Bandpass Modulated Waveforms," *Proc. IEEE Black Sea Conference on Communications and Networking (BlackSeaCom)*, pp.1-5, Jun 2016.

[28] S. Sobolewski, W. L. Adams Jr and R. Sankar, "Recognition of Modern Modulated Waveforms with Applications to ABMS and VDATS TPS Development," *Proc. IEEE AutoTestCon,* Aug 2022. (To Appear)

[29] S. Hong, M. Sagong, C. Lim, K. Cheun and S. Cho, "FQAM: A Modulation Scheme for Beyond 4G Cellular Wireless Communication Systems," *Proc. GlobeCom 2013 Workshop - Emerging Technologies for LTE-Advanced and Beyond 4G*, pp.25-30, 2013.

[30] S. Sidiq, F. Mustafa, J.A. Sheikh and B.A. Malik, " FBMC and UFMC: The Modulation Techniques for 5G," *Proc. IEEE International Conference on Power Electronics, Control and Automation (ICPECA)*, pp.1-5, 2019.

[31] P.N. Rani and C.S. Rani, "UFMC: The 5G Modulation Technique," *Proc. Int'l Conf. on Computational Intelligence and Computing Research*, pp.1-3, 2016.

[32] S. Sobolewski, W. L. Adams Jr and R. Sankar, " Automatic Modulation Recognition Techniques Based on Cyclostationary and Multifractal Features For Distinguishing LFM, PWM and PPM Waveforms Used in Radar Systems as Example of Artificial Intelligence Implementation in Test," *Proc. IEEE AutoTestCon,* pp. 335-340, Sep 2012.

[33] F. He, Y. Yin, L. Zhou, X. Xu and H. Man, "Principal Component Analysis of Cyclic Spectrum Features in Automatic Modulation Recognition," *Proc. IEEE MILCOM*, pp.1737-1742, Oct 2010.

[34] S. Xu, B. Huang, L. Xu and Z. Xu, "Radio Transmitter Classification Using a New Method of Stray Features Analysis Combined with PCA," *Proc. IEEE MILCOM*, pp.1-5, Oct 2007.

[35] J. Kim and Y. Kim, "An Efficient Compression Algorithm Using Variance of Motion Vector," *The 18th IEEE International Symposium on Consumer Electronics (ISCE)*, pp.1-2, 2014.

[36] D. Saupe and S. Jacob, "Variance-based Quadtrees in Fractal Image Compression," Electronic Letters, Vol.33, No.1, Jan 1997.

[37] B. Ramkumar, "Automatic Modulation Classification cfor Cognitive Radios Using Cyclic Feature Detection," *IEEE Circuits and Systems*, Vol.2. No.2, pp.27-45, Second Quarter 2009.

[38] P.A. Forero, A. Cano and G.B. Giannakis, "Distributed Feature-based Modulation Classification Using Wireless Sensor Networks," *Proc. IEEE MILCOM*, pp.1-7, Nov 2008.

[39] L.V. Fausett, "Fundamentals of Neural Networks: Applications, Algorithms and Applications," *Pearson*, pp.461, 1994.

[40] E. Kanterakis and W. Su, "OFDM Signal Classification in Frequency Selective Rayleigh Channels," *Proc. IEEE MILCOM*, pp.1-6, Nov 2011.

Appendix A: Copyright Permissions

The permissions below are for the use of published content used in Chapter 2.

RightsLink

Home | Help | Email Support | Sign in | Create Account

IEEE Requesting permission to reuse content from an IEEE publication

Universal Nonhierarchical Automatic Modulation Recognition Techniques For Distinguishing Bandpass Modulated Waveforms Based On Signal Statistics, Cumulant, Cyclostationary, Multifractal And Fourier-Wavelet Transforms Features

Conference Proceedings: 2014 IEEE Military Communications Conference

Author: Sylwester Sobolewski; William Larry Adams; Ravi Sankar

Publisher: IEEE

Date: 6-8 Oct. 2014

Thesis / Dissertation Reuse

The IEEE does not require individuals working on a thesis to obtain a formal reuse license, however, you may print out this statement to be used as a permission grant:

Requirements to be followed when using any portion (e.g., figure, graph, table, or textual material) of an IEEE copyrighted paper in a thesis:

1) In the case of textual material (e.g., using short quotes or referring to the work within these papers) users must give full credit to the original source (author, paper, publication) followed by the IEEE copyright line © 2011 IEEE.
2) In the case of illustrations or tabular material, we require that the copyright line © [Year of original publication] IEEE appear prominently with each reprinted figure and/or table.
3) If a substantial portion of the original paper is to be used, and if you are not the senior author, also obtain the senior author's approval.

Requirements to be followed when using an entire IEEE copyrighted paper in a thesis:

1) The following IEEE copyright/ credit notice should be placed prominently in the references: © [year of original publication] IEEE. Reprinted, with permission, from [author names, paper title, IEEE publication title, and month/year of publication]
2) Only the accepted version of an IEEE copyrighted paper can be used when posting the paper or your thesis on-line.
3) In placing the thesis on the author's university website, please display the following message in a prominent place on the website: In reference to IEEE copyrighted material which is used with permission in this thesis, the IEEE does not endorse any of [university/educational entity's name goes here]'s products or services. Internal or personal use of this material is permitted. If interested in reprinting/republishing IEEE copyrighted material for advertising or promotional purposes or for creating new collective works for resale or redistribution, please go to http://www.ieee.org/publications_standards/publications/rights/rights_link.html to learn how to obtain a License from RightsLink.

If applicable, University Microfilms and/or ProQuest Library, or the Archives of Canada may supply single copies of the dissertation.

BACK | CLOSE WINDOW

Effective and efficient compound feature vectors applicable to discrimination of any conceivable bandpass modulated waveforms

Requesting permission to reuse content from an IEEE publication

Conference Proceedings:
2016 IEEE International Black Sea Conference on Communications and Networking (BlackSeaCom)

Author: Sylwester Sobolewski; William Larry Adams; Ravi Sankar

Publisher: IEEE

Date: 6-9 June 2016

Thesis / Dissertation Reuse

The IEEE does not require individuals working on a thesis to obtain a formal reuse license, however, you may print out this statement to be used as a permission grant:

Requirements to be followed when using any portion (e.g., figure, graph, table, or textual material) of an IEEE copyrighted paper in a thesis:

1) In the case of textual material (e.g., using short quotes or referring to the work within these papers) users must give full credit to the original source (author, paper, publication) followed by the IEEE copyright line © 2011 IEEE.
2) In the case of illustrations or tabular material, we require that the copyright line © [Year of original publication] IEEE appear prominently with each reprinted figure and/or table.
3) If a substantial portion of the original paper is to be used, and if you are not the senior author, also obtain the senior author's approval.

Requirements to be followed when using an entire IEEE copyrighted paper in a thesis:

1) The following IEEE copyright/ credit notice should be placed prominently in the references: © [year of original publication] IEEE. Reprinted, with permission, from [author names, paper title, IEEE publication title, and month/year of publication]
2) Only the accepted version of an IEEE copyrighted paper can be used when posting the paper or your thesis on-line.
3) In placing the thesis on the author's university website, please display the following message in a prominent place on the website: In reference to IEEE copyrighted material which is used with permission in this thesis, the IEEE does not endorse any of [university/educational entity's name goes here]'s products or services. Internal or personal use of this material is permitted. If interested in reprinting/republishing IEEE copyrighted material for advertising or promotional purposes or for creating new collective works for resale or redistribution, please go to http://www.ieee.org/publications_standards/publications/rights/rights_link.html to learn how to obtain a License from RightsLink.

If applicable, University Microfilms and/or ProQuest Library, or the Archives of Canada may supply single copies of the dissertation.

BACK   CLOSE WINDOW